SUMMARY REPORT OF MISSION ACCELERATION MEASUREMENTS FOR STS-75

Launched February 22, 1996

Authors:

Melissa J. B. Rogers
Tal-Cut Company
Beachwood, Ohio

Kenneth Hrovat
Tal-Cut Company
Beachwood, Ohio

Kevin M. McPherson
Lewis Research Center
Cleveland, Ohio

Milton E. Moskowitz
Tal-Cut Company
Beachwood, Ohio

Richard DeLombard
Lewis Research Center
Cleveland, Ohio

Abstract

Two accelerometers provided acceleration data during the STS-75 mission in support of the third United States Microgravity Payload (USMP-3) experiments. The Orbital Acceleration Research Experiment (OARE) and the Space Acceleration Measurement System (SAMS) provided a measure of the microgravity environment of the Space Shuttle Columbia. The OARE provided investigators with quasi-steady acceleration measurements after about a six hour time lag dictated by downlink constraints. SAMS data were downlinked in near-real-time and recorded on-board for post-mission analysis. An overview of the mission is provided as are brief discussions of these two accelerometer systems.

Data analysis techniques used to process SAMS and OARE data are discussed. Using a combination of these techniques, the microgravity environment related to several different Orbiter, crew, and experiment operations is presented and interpreted. The microgravity environment represented by SAMS and OARE data is comparable to the environments measured by the instruments on earlier microgravity science missions. The OARE data compared well with predictions of the quasi-steady environment. The SAMS data show the influence of thruster firings and crew motion (transient events) and of crew exercise, Orbiter systems, and experiment operations (oscillatory events). Thruster activity on this mission appear to be somewhat more frequent than on other microgravity missions with the combined firings of the F5L and F5R jets producing significant acceleration transients. The specific crew activities performed in the middeck and flight deck, the SPREE table rotations, the waste collection system compaction, and the fuel cell purge had negligible effects on the microgravity environment of the USMP-3 carriers. The Ku band antenna repositioning activity resulted in a brief interruption of the ubiquitous 17 Hz signal in the SAMS data. In addition, the auxiliary power unit operations during the Flight Control System checkout appeared to have a significant impact on the microgravity environment.

Table of Contents

List of Tables

List of Figures

Abbreviations and Acronyms

AADSF	Advanced Automated Directional Solidification Furnace
$accel_{avg}$	root-sum-square of averaged triaxial data
$accel_{RMS}$	root-sum-square of RMS of triaxial data
APU	auxiliary power unit
DSO	Detailed Supplementary Objective
DTO	Development Test Objective
EDO	Extended Duration Orbiter
EST	Eastern Standard Time
FCS	Flight Control System
GMT	Greenwich Mean Time (day/hour:minute:second)
IDGE	Isothermal Dendritic Growth Experiment
k	number of time series intervals used in analysis
LeRC	NASA Lewis Research Center
LVLH	local vertical local horizontal
M	number of points in time series interval used in analysis
MEPHISTO	Material pour L'Etude des Phenomenes Interessant la Solidification sur Terre et en Orbite Experiment
MET	mission elapsed time (day/hour:minute:second)
MPESS	Mission Peculiar Equipment Support Structure
MSFC	NASA Marshall Space Flight Center
OARE	Orbital Acceleration Research Experiment
OMS	orbital maneuvering system
PIMS	Principal Investigator Microgravity Services
POCC	Payload Operations Control Center
PRCS	primary reaction control system
PSD	power spectral density
RCS	reaction control system
RMS	root mean square
SAMS	Space Acceleration Measurement System
SPREE	Shuttle Potential and Return Electron Experiment
TSH	triaxial sensor head
TSS-1R	Tethered Satellite System-1R
USMP-3	third United States Microgravity Payload
VRCS	vernier reaction control system
VV	velocity vector
WCS	waste collection system
X_h, Y_h, Z_h	SAMS coordinate system axes
X_o,Y_o,Z_o	Orbiter structural coordinate system axes
X_{OARE},Y_{OARE},Z_{OARE}	OARE coordinate system axes
X_b,Y_b,Z_b	Orbiter body coordinate system axes
Zeno	Critical Fluid Light Scattering Experiment

Acknowledgments

Tim Reckart of Tal-Cut Company was responsible for the line drawings in and layout of this report. Nissim Lugasy, Tal-Cut Company, prepared computer software for the acquisition and initial processing of OARE data during the STS-75 mission. Gene Liberman and Doug Deutsch, Tal-Cut Company, prepared computer software for the real-time acquisition, correction, and display of SAMS data during STS-75. Ken Hrovat and Milton Moskowitz, Tal-Cut Company and Kevin McPherson, NASA Lewis Research Center, prepared off-line data analysis software for SAMS and OARE data and provided SAMS and OARE data analysis and plots for this report. The entire PIMS team provided acceleration environment interpretation during the mission.

Alan Bachik, Code DF at NASA Johnson Space Center, provided information about the Flight Control System Checkout procedure. Quinn Carelock, Code DF82 at NASA Johnson Space Center, provided information about the Waste Collection System and timing for compaction operations during STS-75. Kenneth J. Welzyn and Edward Litkenhaus of NASA Marshall Space Flight Center, Jeffrey Zelicksen of CAS Inc., and Nestor Voronka of the University of Michigan provided information and data pertinent to operations of the Tethered Satellite System. Kenneth J. Welzyn provided the data for Figure 16. Michael Moses, Code DFG with Rockwell Space Operations Co. at Johnson Space Center, provided thruster firing information. Ku band antenna information was provided by Richard La Brode, Code DF, Rockwell International at Johnson Space Center. Brenda Eliason, with Rockwell International at NASA Johnson Space Center, provided the STS-75 Green Book which summarized the as-run mission activities.

1. Introduction

Microgravity science experiments are conducted on the NASA Space Shuttle Orbiters to take advantage of the reduced gravity environment available in low earth orbit. Accelerometer systems are flown in conjunction with these experiments to record the microgravity environment to which they are subjected. The third United States Microgravity Payload (USMP-3) and the Tethered Satellite System (TSS-1R) flew on the Orbiter Columbia on mission STS-75 from 22 February to 9 March 1996. Two accelerometer systems managed by the NASA Lewis Research Center (LeRC) flew to support the USMP-3 experiments: the Orbital Acceleration Research Experiment (OARE) and the Space Acceleration Measurement System (SAMS).

The Principal Investigator Microgravity Services (PIMS) project at NASA LeRC supports principal investigators of microgravity experiments as they evaluate the effects of varying acceleration levels on their experiments. During the STS-75 mission, PIMS provided real-time displays of the SAMS data to the investigator teams, enabling them to make appropriate parameter adjustment decisions pertaining to their experiments. PIMS also provided OARE data plots to users as the data became available. PIMS was also able to perform specific processing of archived SAMS and OARE data for USMP-3 and TSS-1R investigators so that they could perform in-depth analyses of their experiment results during the mission. Any additional requests for data analysis should be directed to the authors.

This report provides a summary of the microgravity environment of Columbia during the STS-75 mission. Section 2 is a brief overview of the mission. Section 3 gives some details about the accelerometer systems OARE and SAMS, including the real-time data acquisition, processing, and display operations PIMS performed during the mission. Section 4 discusses the specific data analysis techniques that were used to create the plots presented in this report. Section 5 is a discussion of the effects of specific mission and payload activities on the microgravity environment. Appendix A gives instructions on how to access OARE and SAMS data products using the internet. Appendices B and C are SAMS data plots that summarize the acceleration environment for the entire mission. Appendix D is a user response form we request the reader complete and return to the PIMS group as indicated.

2. Mission Overview

At 03:18 p.m. EST on 22 February 1996 the Space Shuttle Columbia launched on the STS-75 mission from NASA Kennedy Space Center. Landing was at Kennedy Space Center on 9 March at 08:58 a.m. EST. In terms of other time conventions used in this report, launch was at Greenwich Mean

Time (GMT) 053/20:18 or mission elapsed time (MET) 000/00:00 and landing was at GMT 069/13:58 or MET 015/17:40. Both GMT and MET are recorded in day/hour:minute:second format. The primary objectives of the STS-75 mission were to develop an understanding of the basic dynamic and electrodynamic processes governing tethered systems (TSS-1R) and to improve our basic knowledge of materials under microgravity conditions (USMP-3). USMP-3 experiments are listed in Table 1. Other payloads on STS-75 are listed in Table 2. The cargo bay configuration for STS-75 is shown in Fig. 1. Six development test objectives (DTO) and nine detailed supplementary objectives (DSO) were accomplished on STS-75; they are listed in Tables 3 and 4. The seven member crew worked on a three shift schedule that collapsed to two shifts after primary TSS-1R operations were complete. The crew members are listed in Table 5.

3. Accelerometer Systems

Two accelerometer systems measured the microgravity and vibration environment of the Orbiter Columbia in support of the USMP-3 experiments, the Orbital Acceleration Research Experiment and the Space Acceleration Measurement System. The features of these systems are discussed below. Additional accelerometers flew as part of the TSS-1R payload. TSS-1R Mission Management should be contacted for additional information.

3.1 Orbital Acceleration Research Experiment

The OARE measures quasi-steady accelerations from below $1x10^{-8}$ g up to $2.5x10^{-3}$ g. The OARE consists of an electrostatically suspended proof mass sensor, an in-flight calibration subsystem, and a microprocessor which is used for in-flight experiment control, processing, and storage of flight data [1-4], see Appendix D. The acceleration sensor's output signal is filtered using a Bessel filter with a cut off frequency of 1 Hz. The output signal is digitized at 10 samples per second and is then processed and digitally filtered with an adaptive trimmean filter prior to electronic storage on-board. During STS-75, a system write fault resulted in the corruption of the data stored electronically within OARE, see Appendix D. The unprocessed data are recorded on the Orbiter payload tape recorder. At regular intervals during the STS-75 mission, the unprocessed OARE data were downlinked from the Orbiter to the MSFC Payload Operations Control Center (POCC). The POCC Data Reduction team transferred files of downlinked data to PIMS computers in the POCC. The PIMS computers processed the OARE data and displayed data for the PIs using the World Wide Web and the POCC video matrix.

The OARE was mounted to the floor of Columbia's cargo bay on a keel bridge, close to the Orbiter center of gravity. The location and orientation of the sensors with respect to the Orbiter structural coordinate system are given in Table 6 and Fig. 2. In this report, the OARE data are presented in terms of the Orbiter body coordinate system. Fig. 3 indicates the difference between the Orbiter body and structural coordinate systems. The subscript b represents the Orbiter body coordinate system. The subscript o is used to indicate the Orbiter structural coordinate system. The OARE data sign convention used here is such that when there is a forward thrust of the Orbiter, it is reported as a negative X_b acceleration. We refer to this convention as being consistent with a frame of reference fixed to the Orbiter. OARE data are available from MET 000/00:10 to 015/21:03. Appendix A describes how these data can be accessed using the internet.

3.2 Space Acceleration Measurement System

The SAMS is used to measure the low-gravity environment of Orbiters in support of microgravity science payloads. STS-75 was the fourteenth SAMS flight on an Orbiter. Two SAMS units flew on STS-75. A SAMS unit consists of up to three remote triaxial sensor heads, connecting cables, and a controlling data acquisition unit with a digital data recording system using optical disks with 200 megabytes of storage capacity per side. On STS-75, one SAMS unit was located on each Mission Peculiar Equipment Support Structure (MPESS) carrier in support of USMP-3 experiments. The unit designated SAMS-1 (also called Unit F) was located on the forward (MPESS-A) carrier and used two triaxial sensor heads to support the AADSF and MEPHISTO experiments. The signals from these two triaxial sensor heads were filtered by low pass filters with cutoff frequencies of 10 Hz (TSH 1A) and 25 Hz (TSH 1B). These signals were then sampled at 50 and 125 samples per second, respectively. TSH 1A data were downlinked in near real-time during the mission and data from TSH 1B were recorded on board using SAMS optical disks.

The unit designated SAMS-2 (also called Unit G) was located on the aft (MPESS) carrier and used three triaxial sensor heads to support the IDGE and Zeno experiments. The signals from these three triaxial sensor heads were filtered by low pass filters with cutoff frequencies of 5 Hz (TSH 2A), 10 Hz (TSH 2B), and 25 Hz (TSH 2C). These signals were then sampled at 50, 50, and 125 samples per second, respectively. Data from TSH 2A and TSH 2C were alternately downlinked or recorded on optical disks on board. Data from TSH 2B were recorded on optical disks. In general, TSH 2C data were downlinked early in the mission, while TSH 2A data were downlinked later in the mission. In this report, the SAMS data are presented in terms of the Orbiter structural coordinate system. The SAMS data sign convention used here is such that when there is a forward thrust of the Orbiter it is recorded as a negative X_o acceleration. We refer to this convention as an inertial frame of reference fixed to a point in space. The orientations and locations of the SAMS heads, with respect to the Orbiter structural coordinate system, are given in Table 7 and Fig. 4. More detailed descriptions of the SAMS accelerometers are available in the literature [5-10].

The SAMS data that were downlinked were routed to PIMS computers in the POCC. The PIMS computers processed the SAMS data from both units and displayed data for experiments using the World Wide Web and the POCC video matrix. Additionally, Teledyne Brown Engineering personnel modified SAMS data display software so that the crew could capture the SAMS data stream and display it on a laptop computer. The display was a scrolling plot of ten seconds of the three axes of one unit of SAMS data, with a delay of about 20 seconds. This was the first time an Orbiter crew was able to use SAMS data to get real-time feedback on the effects of their activities and Orbiter operations on the microgravity environment. In response to their use of this system, Franklin Chang-Diaz, the Payload Commander, said

> The application was easy to use and useful for crew feedback. It influenced our activities greatly and made us much more aware of the potential crew- induced disturbances. It is a great on-orbit training tool for crews to develop an efficient low-g way of doing things. It also shows that we can do effective work without interfering with micro-g operations (which we thought, but couldn't prove), at least to the level of 100 micro-gs (well inside the vernier orbiter jets but requiring much more care if gravity gradient, free-drift ops were required).

For STS-75, a total of approximately 3.5 gigabytes of SAMS data are available between MET 000/02:57 and 014/11:13. Appendix A describes how these data can be accessed using the internet.

4. SAMS and OARE Data Analysis

The data recorded by SAMS on STS-75 were processed to correct for pre-mission bias calibration offsets and to compensate for temperature and gain related errors of bias, scale factor, and axis misalignment. The resulting units of acceleration are g's where 1 g = 9.8 m/s^2. The data were orthogonally transformed from the five SAMS TSH coordinate systems to the Orbiter structural coordinate system. The OARE data recorded during STS-75 and presented here have been compensated for temperature, bias, and scale factors.[11]

After this initial data correction phase, additional data analyses were applied to the SAMS and OARE data to characterize the acceleration environment of the mission. The analysis techniques used to produce the plots in this report are discussed here. Because of the inherent differences between OARE (frequency range 10^{-5} Hz to 1 Hz, sampling rate 10 samples per second) and SAMS (frequency range 0.01 Hz to 25 Hz, sampling rate 50 to 125 samples per second on STS-75) data, some data analysis techniques are more applicable to data from one system than the other. The particular processing technique used also depends on the type of information desired.

4.1 Time Domain Analysis

The time domain analysis techniques used in this report are acceleration versus time, interval average acceleration versus time, and interval root mean square (RMS) acceleration versus time. For OARE time domain analysis, plots of trimmean acceleration versus time and three-dimensional projections of the data are provided. Some discussion is given in [11] regarding the application of different averaging techniques to OARE data. The notation for all the data analysis discussed here is defined in the Abbreviations and Acronyms list.

SAMS Acceleration versus Time: These are plots of the acceleration in units of g versus time. Among the time domain plots displayed in this report, this one yields the most precise accounting of the variation of acceleration magnitude as a function of time.

SAMS Interval Average Acceleration versus Time: A plot of this quantity in units of g versus time gives an indication of net accelerations which last for a number of seconds equal to or greater than the interval parameter. The interval parameter used for STS-75 data analysis was ten seconds. Shorter duration, high amplitude accelerations can also be detected with this type of plot, however, the exact timing and magnitude of specific acceleration events cannot be extracted. The interval average acceleration for generic x-axis data is defined as

$$x_{avg_k} = \frac{1}{M} \sum_{i=1}^{M} x_{(k-1)M+i}.$$

Corresponding expressions for y- and z-axis data can be combined with that for the X-axis to form the interval average acceleration vector magnitude as follows:

$$\mathrm{accel}_{\mathrm{avg}_k} = \sqrt{x_{\mathrm{avg}_k}^{2} + y_{\mathrm{avg}_k}^{2} + z_{\mathrm{avg}_k}^{2}}.$$

SAMS Interval Root Mean Square Acceleration versus Time: A plot of this quantity in units of g_{RMS} versus time gives a measure of the energy in the acceleration signal due to purely oscillatory acceleration sources. Again, the interval parameter used for STS-75 data analysis was ten seconds. The interval RMS acceleration for generic x-axis data is defined as

$$x_{RMS_k} = \sqrt{\frac{1}{M}\sum_{i=1}^{M}\left(x_{(k-1)M+i}\right)^2}.$$

Corresponding expressions for y- and z-axis data can be combined with that from the X-axis to form the interval RMS acceleration vector magnitude as follows:

$$\mathrm{accel}_{\mathrm{RMS}_k} = \sqrt{x_{\mathrm{RMS}_k}{}^2 + y_{\mathrm{RMS}_k}{}^2 + z_{\mathrm{RMS}_k}{}^2}.$$

OARE Trimmean Acceleration versus Time: A trimmean filter is applied to OARE data to reject transient, higher magnitude accelerations from analysis that is concerned with the quasi-steady environment. This filtering procedure ranks the collected data in order of increasing magnitude, measures the deviation of the distribution from a normal distribution, and deletes (trims) an adaptively determined amount of the data. The mean of the remaining data is calculated and this value is assigned to the initial time of the interval analyzed. For this report the trimmean filter was applied to fifty seconds of OARE data every twenty-five seconds.

Three-dimensional Projection: This type of analysis results in a visualization of the acceleration vector alignment, projected onto three orthogonal planes, for example the top, front, and side view of the Orbiter. The time series is analyzed using a two-dimensional histogram method where the percentage of time the acceleration vector magnitude falls within a two-dimensional bin is plotted as a color. Areas showing colors toward the red end of the colorbar indicate a higher number of occurrences of the acceleration vector magnitude falling within that area. Conversely, areas showing colors toward the blue end are indicative of a lower number of occurrences. This type of plot provides overview information about the total time period analyzed. Exact timing of acceleration events cannot be extracted from this type of plot.

4.2 SAMS Frequency Domain Analysis

Transformation of data to the frequency domain is typically done to gain more insight about the environment and to identify potential acceleration sources. The SAMS frequency domain analysis and displays used in this report are acceleration power spectral density (PSD) versus frequency and acceleration power spectral density versus frequency versus time (spectrogram).

SAMS Power Spectral Density versus Frequency: Spectral analysis is performed on time series data to identify the relative magnitudes of sinusoidal signals that compose the series. The basis of this computation is the Fourier transform which indicates the magnitude of each frequency (sinusoid) present in the time history signal. The PSD is computed directly from the Fourier transform of a time series so that Parseval's Theorem is satisfied: the RMS of a time signal is equal to the square root of the integral of the PSD across the frequency band represented by the original signal. The PSD is reported in units of g^2/Hz.

Welch's Averaged Periodogram Method, or spectral averaging, is often used to produce PSDs that represent the average spectral content of a time period of interest. The PSD of k successive intervals is calculated and the k resulting spectral series are averaged together on a point by point basis.

SAMS Power Spectral Density versus Frequency versus Time (Spectrogram): Spectrograms provide a roadmap of how acceleration signals vary with respect to both time and frequency. As such, they are particularly useful in identifying when certain activities begin and end and to get a general feel for changes in the microgravity environment with time. To produce a spectrogram, PSDs are computed for successive intervals of time. The PSDs are oriented vertically on a page such that frequency increases from bottom to top. PSDs from successive time slices are aligned horizontally across the page such that time increases from left to right. Each time-frequency bin is imaged as a color corresponding to the logarithm of the PSD magnitude at that time and frequency. A color bar is included with each plot as a key to the color to $\log_{10}$(PSD) correspondence. To maximize the value of individual PIMS analyses, spectrogram color bars may vary among analyses and among mission reports. For ease of interpretation, however, within a mission report the color maps are kept constant unless otherwise noted.

5. Columbia Microgravity Environment—STS-75

This section discusses the microgravity environment of the Orbiter Columbia during the STS-75 mission as recorded during a specific crew activity that was performed for environment characterization, during several thruster firing events, during SPREE rotary table operations, during a Ku band antenna repositioning, during Flight Control System checkout, during the Tethered Satellite System deploy and tether break, during a Waste Collection System compaction operation, during a fuel cell purge, and while the Orbiter was positioned in different attitudes. The Appendices provide an overview of the microgravity and vibration environment during the STS-75 mission. Appendix B shows time history and frequency domain representations of SAMS Unit F TSH 1B (25 Hz filter cutoff) data. Appendix C provides time history and frequency domain representations of the SAMS Unit G TSH 2C data (25 Hz filter cutoff).

5.1 Crew Quiet Time Test

Prior to the mission, the crew members were interested in performing specific activities to demonstrate how they can operate quietly to minimize crew disturbances to the microgravity environment. Conversations with STS-75 crew members and mission planners resulted in a suite of activities that were performed during a block of time between TSS-1R operations and the USMP-3 microgravity science operations. After the mission, correlation between the SAMS data and the activities performed by the crew were determined using video tape and crew notations of the activities.

The activities were conducted from MET 006/15:00 to 006/15:37. The activities included normal crew actions involving the middeck lockers, galley equipment, crew equipment (bunks, footloops, and cameras), the waste collection system, crew motions, cabin air fans, and thruster operations. The crew members were basically quiet during this demonstration time. Figure 14 of Appendix B is a spectrogram containing SAMS Unit F TSH 1B data collected during this period. There is no apparent correlation between the crew activities and the SAMS data. Note, however, that with the SAMS sensors located on the MPESS carriers, these data indicate how the activities of the crew in the middeck and flight deck of the Orbiter affected the microgravity environment at the location of the sensitive USMP-3 experiments. The data do not represent what the environment was at the site of the activity and we can draw no conclusions about the effects of these same activities on the acceleration environment of the middeck, flight deck, or of a Spacelab module that may house sensitive experiments while such activities are occurring in the Orbiter.

5.2 Attitude Adjustment and Maintenance

Orbiter attitude adjustment and maintenance is performed using the Reaction Control System (RCS) and the Orbital Maneuvering System (OMS). STS-75 provided several opportunities to investigate the effects of the use of these systems on the microgravity environment.

Examination of the ten second interval average plots in Appendices B and C reveals a somewhat regular train of short-duration, high-magnitude disturbances most notable in the Orbiter Z_o-axis data and, to a lesser extent, in the X_o-axis data. Correlation of SAMS data from MET 010/04 with Orbiter downlink data confirmed that these disturbances were induced when two Vernier Reaction Control System (VRCS) thrusters (F5L and F5R) were fired simultaneously as required for attitude maintenance with a 1° deadband. See reference [12] for identification of individual RCS jets. Fig. 5 shows SAMS Unit F TSH 1B data with a ten second interval average calculation applied. In Fig. 5 the simultaneous firing of the two thrusters is indicated by the + markers. Note from the o markers that firing either of these thrusters individually leaves little or no evidence in the interval average data. However, when fired in tandem there is an appreciable momentary shift in the DC acceleration levels as evidenced on the X_o- and Z_o-axes.

The USMP-3 experiment MEPHISTO focused on mass transport in directionally solidifying Sn-Bi alloys. Part of their experiment was a benchmark study to correlate well-defined acceleration conditions with well-controlled solidification conditions. The acceleration sources used for this study were nine Primary RCS (PRCS) firings, one OMS firing, and one Orbiter roll maneuver. SAMS Unit F TSH 1B data from three of the PRCS firings are shown in Figs. 6-8. Note that because the sign convention for the X and Z axes are opposite for the Orbiter structural and body coordinate systems, the $-Z_b$ burn of Fig. 6 causes a shift in the $+Z_o$ direction. Reference 12 discusses several PRCS and OMS firings that occurred during STS-75, some of which are the MEPHISTO activities. Table 8 compares acceleration level shifts as seen in the SAMS data to dV/dt values obtained from Reference 13. While the exact provenance of the dV/dt values are unclear, the correlation shown in the table is significant.

Figure 9 is provided as a more detailed view of the accelerations associated with one of the MEPHISTO PRCS events. The fifteen second $-Z_b$ axis PRCS 5D maneuver was performed at MET 012/12:25 using the PRCS thrusters L2D, L3D, R2D, R3D, F3D, and F4D [13]. As seen by the six discretes at the top of Fig. 9, two of the forward thrusters (F3D, F4D) were fired for the entire fifteen second burn. The Y-axis components of these two jets negated each other and the Z-axis components were additive. This action translated the nose of the Orbiter in the $-Z_b$ direction, while the tail was translated in the $-Z_b$ direction by firing 4 aft jets (L2D, L3D, R2D, R3D). Note that the aft jets were not fired continuously and these transients are clearly seen in the SAMS Z_o data in Fig. 9.

5.3 SPREE Rotary Table Operations

The TSS-1R Shuttle Potential and Return Electron Experiment (SPREE) was designed to measure the charged particle populations around the Orbiter. SPREE was mounted on the port side of the TSS-1R MPESS. The sensors for SPREE were two pairs of electrostatic analyzers, each pair mounted on a rotary table motor drive. These tables were configured to rotate at one revolution per minute.

During STS-75, the SPREE experiment team requested to perform experiments that required the tables rotate during USMP-3 microgravity periods. A series of tests were performed to determine whether or not the rotation of the heads had a deleterious effect on the microgravity environment. During an Orbiter free drift period, the two rotating tables were parked and rotated at 1 rpm as indicated in Table 9. Fig. 10 shows SAMS Unit F, Head 1B data collected during these activities. The table rotation rate translates to a frequency of ~0.02 Hz. No notable accelerations are seen in the data. Nor are there any evident transients in the data when the table rotations were initiated or ceased. This was analyzed by PIMS during the mission and because there were no evident accelerations related to the SPREE rotations, the USMP-3 Mission Scientist permitted these activities to occur as needed during the microgravity periods. OARE data are not available for this time period because of OARE instrument calibrations operations.

5.4 Ku band Antenna Repositioning

The Ku band antenna on the Orbiters is used to transmit data and voice communications between the Orbiters and ground stations via the Tracking and Data Relay Satellite System satellites [14]. The Ku band deployed assembly is mounted on the starboard sill of the payload bay. It is deployed and activated after the payload bay doors are opened. The antenna dish is edge-mounted on a two-axis gimbal. The alpha gimbal provides a 360° roll movement around the pole of the gimbal. The beta gimbal provides a 162° pitch movement around its axis. The alpha gimbal has a stop at the lower part of its movement to prevent wraparound of the beta gimbal control cable. Periodically the Ku band antenna beta cabling requires positioning to ensure that it does not become twisted in a way that could cause the antenna to bind. This gimbal flip is achieved by a fast slew of the antenna dish in the direction needed to unwrap the cable.

Figure 11 shows a spectrogram generated from SAMS Unit F TSH 1B data for a period in which the Ku band antenna was repositioned. In this figure, the 17 Hz acceleration signal characteristic of the antenna's dither frequency stops at MET 007/13:05:25, and resumes approximately 17 seconds later. This break in the usually continuous 17 Hz signal is related to the repositioning activity. During fast slew operations, the 17 Hz dither is disabled.

5.5 Flight Control System Checkout

Approximately one day before scheduled re-entry, a two-part checkout procedure is performed to verify operations of the Orbiter Flight Control System (FCS). The first part of this checkout uses one of the three Auxiliary Power Units (APUs) to circulate hydraulic fluid in order to move the rudder, elevons, and ailerons of the Orbiter. As an APU is activated, exhaust gas is vented in the $-Z_b$ direction. The result of this venting is similar in nature to a VRCS jet firing, ranging from nearly 0 to 30 pounds of force. The exhaust does not vent as a steady stream, but cycles at approximately 1 to 1.5 Hz.

Typically, part one of the FCS checkout lasts for 5-9 minutes, but the STS-75 checkout lasted for approximately 25 minutes. The test was prolonged so that Johnson Space Center personnel could troubleshoot an FCS channel failure. Fig. 12 is a SAMS Unit G TSH 2A spectrogram showing the extent of the first part of the FCS checkout. The activation of APU1 is identified in the plot at about 013/15:03 by a sudden change in acceleration characteristics. Of particular note is the appearance of a 1.3 Hz signal and several upper harmonics. These signals remain in the data throughout the checkout period, with slight shifts in the frequencies about 13 and 18 minutes into the plot. Broadband excitation of the microgravity environment about four minutes into the plot appear to be correlated with changes in APU1 turbine activity as are shorter excitations between 013/15:20 and 013/15:27. The PIMS team is working with Johnson Space Center personnel to resolve the exact correlation between the APU1 operations and the disturbances in the acceleration data.

Part two of the FCS checkout procedure tests various Orbiter electronics systems and should not cause a measurable disturbance to the microgravity environment.

5.6 TSS-1R Operations

The USMP-3 investigators were very interested in how the deployment of the TSS-1R satellite would affect the quasi-steady environment of Columbia. In particular, the IDGE team planned to take advantage of the unique microgravity conditions afforded by the full deployment of the satellite to complete a matrix of investigations that could not be performed on the ground or in the standard Orbiter configurations. OARE data shown in Fig. 13 depict the quasi-steady environment of the Orbiter at the OARE location for a six hour period encompassing TSS deploy operations. This plot indicates the microgravity levels prior to TSS Satellite deploy, during the flyaway and deploy phases, at the time of the tether break, and after the tether break.

From an average acceleration level of X_b=0.08 micro-g, Y_b=-0.18 micro-g, Z_b=0.67 micro-g in the Orbiter deploy attitude, PYR=(210, 10, 188), the environment changed to X_b=-18 micro-g, Y_b=-0.1 micro-g, Z_b=37 micro-g at the time of the tether separation. The raw OARE data took approximately 49 seconds to return to nominal levels after the tether break. The shift in acceleration levels indicated here is consistent with predictions of the quasi-steady environment with the satellite deployed to 20 km.

Figs. 14 and 15 are two different representations of SAMS data collected during the satellite deploy activities. Fig. 14 shows SAMS Unit F TSH 1A data with the signal processed using a thirty second interval average. Fig. 15 is a spectrogram of SAMS Unit F TSH 1A data for the deploy time. Transient accelerations at about 003/01:40 and between 003/02:00 and 003/03:00 appear in Figs. 13-15. These are related to Orbiter maneuvers during the TSS deploy operations. A series of transients at about 003/01:20 is caused by RCS activity, activated to compensate for TSS dynamics. In the spectrogram there is a band of disturbances that starts between 5 and 10 Hz and ranges up to about 20 Hz. These disturbances appear to correspond to the speed of the deploying TSS cable, Fig. 16. The speed of the cable was varied during deployment for experimental investigations and because of coupled TSS and Orbiter dynamics. According to information from the TSS investigators, the TSS deploy apparatus in the Orbiter cargo bay has multiple pulleys of various sizes (in the range of 5 to 15 cm diameter) to guide the cable. These pulleys' rotational rates dependent on the cable speed which varied between 0 and 2.2 meters per second. Frequencies of about 6 Hz are consistent with calculations of disturbance frequencies using nominal values for the size of pulleys and the cable speed. Multiple pulleys of various sizes could correspond to the multiple traces in the SAMS spectrogram of Fig. 15. Figure 17 shows the response of SAMS Unit F TSH 1A to the break of the TSS tether. The initial response to the break is a ringing at about 9 Hz.

5.7 Waste Collection System Compaction

The waste collection system is a multifunctional system used primarily to collect and process biological waste from crew members. This system is located in the Orbiter middeck. Some of its functions include collecting, storing, and drying fecal wastes and associated tissues; processing urine and transferring it to the waste water tank; and venting trash container gases overboard. Within the waste collection system is a compactor device which is used to increase the commode capacity. Compaction is typically performed once per flight. The compactor is manually driven using a ratchet wrench. A mobile vane is rotated around on the radius of the commode. Because the compactor only collects and compacts what is already collected in the commode, compaction should not affect venting from the waste collection system vacuum vent. The waste compaction operation was performed at approximately 009/01:32 during STS-75. Fig. 18 shows SAMS data collected during this time. The compaction apparently does not disturb the acceleration environment out on the MPESS carriers. OARE data from that time frame indicate no apparent venting forces are associated with the compaction operation.

5.8 Fuel Cell Purge

The three fuel cell power plants, through chemical reactions, generate all of the 28-volt direct-current electrical power for the Orbiters from launch through landing [14]. The fuel cells are located under the payload bay area in the forward portion of the Orbiter's midfuselage. The cells contain an electrolyte consisting of potassium hydroxide and water, an oxygen electrode (cathode), and a hydrogen electrode (anode). The fuel cell power plants generate heat and water as by-products of electrical power generation. The water is directed to the potable water storage subsystem. If the water tanks are full or there is line blockage, the water is vented overboard through the water relief line and nozzle. This vent is indicated in Fig. 19 (FCP water relief) which is an overview of the Orbiter on-board venting locations.

During normal fuel cell operation, it is necessary to cleanse the cells at least twice daily to purge contaminants. When a purge is initiated by opening the purge valves, the oxygen and hydrogen systems become open-loop and the increased flows allow the reactants to circulate, pick up contaminants, and blow them overboard through purge lines and vents. H_2 and O_2 purging occurs concurrently, and the venting is directed so that the only non-compensated thrust is in the Orbiter Y-axis direction. There were no apparent disturbances seen in the OARE data associated with a fuel cell purge at 011/02:54. Figs. 31a, 31b, and 32 of Appendix B show SAMS Unit F TSH 1B data collected during this fuel cell purge. There are no apparent disruptions in the SAMS data associated with this activity.

5.9 Orbiter Attitude

During the course of an Orbiter mission, the Orbiter vehicle is controlled to maintain certain parameters, such as pointing, rotation rates, or attitudes. These parameters are customarily defined by the primary payload(s) of a particular mission, the Orbiter program office, the crew office, and the safety office. For a typical microgravity science mission, the attitude is maintained to optimize certain secondary parameters, such as the net quasi-steady acceleration, duration and frequency of thruster firings, and the number of attitude changes during the course of the mission.

The STS-75 mission had several primary attitudes defined for the TSS-1R and USMP-3 payloads. There were a variety of attitudes and Orbiter maneuvers before the tethered satellite deployment and after the tether separation during the first five days of the mission. The basic attitude flown while the tethered satellite was being deployed was the +ZLV/-XVV attitude. Table 10 lists some of the attitudes from STS-75. The as-flown attitude timeline should be consulted for detailed times and attitude parameters [13].

The attitude flown for the USMP-3 payload during the majority of the last eight days of the mission (MET 005/00:15 to 013/14:00) was a gravity gradient attitude -XLV/+ZVV (PYR~95,5,0). This USMP-3 default attitude was chosen to minimize attitude changes, the number of thruster firings, and to reduce the possibility of Orbiter debris damage. Variations in the microgravity environment due to Orbiter attitudes are best seen in the OARE data. Fig. 20 is a plot of OARE data for the entire STS-75 mission. Fig. 21 is an example of the quasi-steady environment related to the nominal USMP-3 attitude.

Three different attitudes were flown during processing of the three AADSF samples on MET days 008, 009, and 010, Table 10. These AADSF attitudes were designed to result in a quasi-steady vector in line with, against, and transverse to the crystal growth direction. The resulting quasi-steady environment associated with each of these attitudes is represented in Figs. 22-27. Specific attitudes flown for MEPHISTO operations are listed in Table 10. Specific thruster firings for the MEPHISTO experiment are discussed in Section 5.2.

For other discussions on the effects of attitudes and attitude changes on the microgravity environment, see [10,12].

6. Summary

The microgravity environment of the Space Shuttle Columbia was measured during the STS-75 mission using accelerometers from two different instruments, OARE and SAMS. The OARE provided USMP-3 investigators with quasi-steady acceleration measurements after about a six hour time lag dictated by downlink constraints. SAMS data were downlinked in near-real-time in support of the USMP-3 investigators and recorded on-board for post-mission analysis.

The standard data analysis techniques used to process SAMS and OARE data are discussed. Using a combination of these techniques, the microgravity environment related to several different Orbiter, crew, and experiment operations is presented and interpreted. SAMS data are analyzed to determine the effects of specific crew activities, Reaction Control System jet firings, SPREE experiment table rotations, a Ku band antenna repositioning, the Flight Control System checkout, Tethered Satellite System deploy activities, a Waste Collection System compaction, and a fuel cell purge. OARE data are analyzed for the same SPREE, TSS-1R, WCS, and fuel cell purge operations and for times with different Orbiter attitudes.

The specific crew activities performed in the middeck and flight deck, the SPREE table rotations, the WCS compaction, and the fuel cell purge had negligible effects on the microgravity environment of the USMP-3 MPESS carriers. Of particular note in the analysis of VRCS data is that the F5L and F5R jets when fired in tandem caused appreciably higher magnitude accelerations than expected based on the magnitudes of single firings. The Ku band repositioning activity resulted in a brief interruption of the ubiquitous 17 Hz signal in the SAMS data.

The STS-75 microgravity environment represented by SAMS and OARE data is comparable to the environments measured by the instruments on earlier microgravity science missions. The OARE data compared well with predictions of the quasi-steady environment and, therefore, must be accurately representing this regime of the environment. OARE measures actual accelerations, so the effects of venting operations such as water dumps and flash evaporator system activities which are not shown in predictions can be seen in this data set. The SAMS data from STS-75 show the influence of thruster firings (transient events) and of crew exercise and Orbiter systems and experiment operations (oscillatory events). VRCS activity on this mission appear to be somewhat more frequent than on other microgravity missions with the combined firings of the F5L and F5R jets producing significant acceleration transients. Orbiter structural modes and crew exercise frequencies are typically the same among Orbiters, missions, and crew members. The main differences among missions are the specific frequencies of equipment oscillations. Better coordination between PIMS and experiment and Orbiter systems designers and engineers is needed to help identify the sources of all distinct characteristics of the Orbiter microgravity environment. For STS-75, we have expanded our understanding of the effects of Orbiter operations on the environment by investigating the Ku band antenna repositioning, WCS compaction, fuel cell purges, and FCS checkout activities. Of these, only the APU operations during the FCS checkout appeared to have a significant impact on the microgravity environment.

7. References

[1] Blanchard, R. C., M. K. Hendrix, J. C. Fox, D. J. Thomas, and J. Y. Nicholson, Orbital Acceleration Research Experiment. J. Spacecraft and Rockets, Vol. 24, No. 6, (1987) 504 - 511.

[2] Blanchard, R. C., J. Y. Nicholson, and J. R. Ritter, STS-40 Orbital Acceleration Research Experiment Flight Results During a Typical Sleep Period. NASA Technical Memorandum 104209, January 1992.

[3] Blanchard, R. C., J. Y. Nicholson, J. R. Ritter, Preliminary OARE Absolute Acceleration Measurements on STS-50. NASA Technical Memorandum 107724, February 1993.

[4] Blanchard, R. C., J. Y. Nicholson, J. R. Ritter, and K. T. Larman, OARE Flight Maneuvers and Calibration Measurements on STS-58. NASA Technical Memorandum 109093, April 1994.

[5] DeLombard, R., B. D. Finley, Space Acceleration Measurement System description and operations on the First Spacelab Life Sciences Mission. NASA Technical Memorandum 105301, November 1991.

[6] DeLombard, R., B. D. Finley, and C. R. Baugher, Development of and flight results from the Space Acceleration Measurement System (SAMS). NASA Technical Memorandum 105652, January 1992.

[7] Baugher, C. R., G. L. Martin, and R. DeLombard, Low-frequency vibration environment for five shuttle missions, NASA Technical Memorandum 106059, March 1993.

[8] Rogers, M. J. B., C. R. Baugher, R. C. Blanchard, R. DeLombard, W. W. Durgin, D. H. Matthiesen, W. Neupert, and P. Roussel, A Comparison of low-gravity measurements onboard Columbia during STS-40. Microgravity Science and Technology VI/3 (1993) 207 - 216.

[9] Finley, B. D., C. Grodsinsky, and R. DeLombard, Summary report of mission acceleration measurements for SPACEHAB-01, STS-57. NASA Technical Memorandum 106514, March 1994.

[10] Summary report of mission acceleration measurements for STS-73. NASA Technical Memorandum 107269, July 1996.

[11] Rice,J.E., OARE Technical Report #148, OARE STS-75 (USMP-3) Final Report, CSI-9603, June 1996.

[12] DeLombard, R., Compendium of information for interpreting the microgravity environment of the orbiter spacecraft, NASA Technical Memorandum 107032, August 1996.

[13] STS-75 Space Shuttle Mission Report, NSTS-37406, Johnson Space Center, April 1996

[14] Shuttle Operational Data Book, Volume 1, JSC-08934, Rev. E, Johnson Space Center, Houston, TX, January 1988.

Table 1. USMP-3 Experiments

Experiments	*Location*	*Contact*	*Affiliation*
Advanced Automated Directional Solidification Furnace (AADSF)	MPESS	Linda B Jeter	NASA Marshall Space Flight Center, Huntsville, AL
Critical Fluid Light Scattering Experiment (Zeno)	MPESS	Richard W. Lauver	NASA Lewis Research Center Cleveland, OH
Isothermal Dendritic Growth Experiment (IDGE)	MPESS	Edward A.Winsa	NASA Lewis Research Center Cleveland, OH
MEPHISTO	MPESS	Gerard Cambon	Centre National d'Etudes Spatiales (CNES) Toulouse, France
Forced-Flow Flamespreading Test (FFFT)	Middeck	Kurt R. Sacksteder	NASA Lewis Research Center Cleveland, OH
Radiative Ignition and Transition to Spread Investigation (RITSI)	Middeck	Sandra Olsen	NASA Lewis Research Center Cleveland, OH
Comparative Soot Diagnostics (CSD)	Middeck	David L. Urban	NASA Lewis Research Center Cleveland, OH
Space Acceleration Measurement System (SAMS)	MPESS	Ronald Sicker	NASA Lewis Research Center Cleveland, OH
Orbital Acceleration Research Experiment (OARE)	Keel Bridge	William Wagar	NASA Lewis Research Center Cleveland, OH

Table 2. STS-75 Payloads

Payloads	*Location*	*Contact*	*Affiliation*
Third United States Microgravity Payload (USMP-3)	Cargo Bay	Sherwood Anderson	NASA Marshall Space Flight Center, Huntsville, AL
Tethered Satellite System (TSS)	Cargo Bay	Robert McBrayer	NASA Marshall Space Flight Center, Huntsville, AL
Middeck Glovebox (MGBX)	Middeck	Sherwood Anderson	NASA Marshall Space Flight Center, Huntsville, AL

Table 3. STS-75 Developmental Test Objectives

DTO 301D	Ascent Structural Capability Evaluation
DTO 307D	Entry Structural Capability
DTO 312	ET TPS Performance
DTO 319D	Orbiter/Payload Acceleration and Acoustics Environment Data
DTO 667	Portable In-Flight Landing Operations Trainer
DTO 805	Crosswind Landing Performance

Table 4. STS-75 Detailed Supplementary Objectives

DSO 331	Interaction of the Space Shuttle Launch and Entry Suit and Sustained Weightlessness on Egress Locomotion
DSO 487	Immunological Assessment of Crew Members
DSO 491	Characterization of Microbial Transfer Among the Crew
DSO 492	In-Flight Evaluation of a Portable Clinical
DSO 493	Monitoring Latent Virus Reactivation and Shedding in Astronauts
DSO 802	Educational Activities
DSO 901	Documentary Television
DSO 902	Documentary Motion Picture Photography
DSO 903	Documentary Still Photography

Table 5. STS-75 Crew

Crewmember	***Position***
Andrew M. Allen	Commander
Scott J. Horowitz	Pilot
Franklin R. Chang-Diaz	Payload Commander
Maurizio Cheli	Mission Specialist 1, ESA
Jeffrey A. Hoffman	Mission Specialist 2
Claude Nicollier	Mission Specialist 3, ESA
Umberto Guidoni	Payload Specialist 1

Table 6. STS-75 OARE Head Location and Orientation

OARE Sensor		Sample Rate: 10 samples/second
Location: Orbiter Cargo Bay Keel Bridge		Frequency: 0 to 1 Hz
ORIENTATION		**LOCATION**
Orbiter Structural Axis	**Sensor Axis**	**Structural Axis**
X_o	$-X_{OARE}$	X_o = 1153.3 in
Y_o	Z_{OARE}	Y_o = -1.3 in
Z_o	Y_{OARE}	Z_o = 317.8 in

Table 7. STS-75 SAMS Head Location and Orientation

Unit F Head 1A (TSH-1A)		Sample Rate: 50 samples/second
Serial no.: 821-19		
Location: Forward MPESS, Forward rail		Frequency: 10 Hz
ORIENTATION		**LOCATION**
Orbiter Structural Axis	**Sensor Axis**	**Structural Axis**
X_O	$-Y_H$	X_O = 1048.37 in
Y_O	$+Z_H$	Y_O = 4.82 in
Z_O	$-X_H$	Z_O = 418.13 in

Unit F Head 1B (TSH-1B)		Sample Rate: 125 samples/second
Serial no.: 821-21		
Location: Forward MPESS, Forward rail		Frequency: 25 Hz
ORIENTATION		**LOCATION**
Orbiter Structural Axis	**Sensor Axis**	**Structural Axis**
X_O	$-Y_H$	X_O = 1048.37 in
Y_O	$+Z_H$	Y_O = -4.73 in
Z_O	$-X_H$	Z_O = 418.13 in

Unit G Head 2A (TSH-2A)		Sample Rate: 50 samples/second
Serial no.: 821-4		
Location: Inside IDGE, (aft MPESS)		Frequency: 5 Hz
ORIENTATION		**LOCATION**
Orbiter Structural Axis	**Sensor Axis**	**Structural Axis**
X_O	$-X_H$	X_O = 1135.42 in
Y_O	$+Y_H$	Y_O = -45.24 in
Z_O	$-Z_H$	Z_O = 433.96 in

Table 7. STS-75 SAMS Head Location and Orientation (cont.)

Unit G Head 2B (TSH-2B) Serial no.: 821-29 Location: Aft MPESS, Aft rail		Sample Rate: 50 samples/second Frequency: 10 Hz
ORIENTATION		**LOCATION**
Orbiter Structural Axis	**Sensor Axis**	**Structural Axis**
X_O	$+Y_H$	X_O = 1136.82 in
Y_O	$-Z_H$	Y_O = -4.82 in
Z_O	$-X_H$	Z_O = 418.13 in

Unit G Head 2C (TSH-2C) Serial no.: 821-20 Location: Aft MPESS, Aft rail		Sample Rate: 125 samples/second Frequency: 25 Hz
ORIENTATION		**LOCATION**
Orbiter Structural Axis	**Sensor Axis**	**Structural Axis**
X_O	$+Y_H$	X_O = 1136.82 in
Y_O	$-Z_H$	Y_O = 4.73 in
Z_O	$-X_H$	Z_O = 418.13 in

Table 8. Accelerations Associated with PRCS Activity

firing	**Average acceleration (from plot)**	**dV/dt [12]**
OMS-3	46 mg	50 mg
PRCS 5D	11 mg	14 mg
PRCS 5C1	6 mg	6 mg
PRCS 5C2	7 mg	6 mg

Table 9. SPREE Rotary Table Operation Times

004/11:11:39	Park head A
004/11:13:46	Rotate head A
004/11:14:10	Park head B
004/11:16:31	Park head A
004/11:18:37	Rotate head A
004/11:18:47	Rotate head B

Table 10. Subset of STS-75 As-flown Attitude Timeline

MET Start	***MET End***	***Attitude***	***Event***
000/00:00	005/00:00	various	TSS Operations
005/01:08	013/14:30		various -XLV/+XVV USMP-3 Operations
005/00:15	005/01:08	various	SAMS Calibration Maneuvers
005/05:15	005/10:30	various	AADSF attitude calibration
005/21:00	005/21:45	LVLH R = 90.0 P = 180.0 Y = 0.0	-YLV/-XVV Sample settling, RCS burn for MEPHISTO operations
005/21:45	005/21:55		Freedrift
005/21:55	005/23:15	LVLH R = 90.0 P = 180.0 Y = 0.0	MEPHISTO sample settling
005/23:15	006/00:00	LVLH R = 290.92 P = 91.61 Y = 357.95	BIAS -XLV/-YVV Sample settling, RCS burn for MEPHISTO Operations
006/00:00	006/00:10		Freedrift

Table 10. Subset of STS-75 As-flown Attitude Timeline (cont.)

006/00:10	006/02:00	LVLH R = 290.92 P = 91.61 Y = 357.95	BIAS -XLV/-YVV Sample settling MEPHISTO operations
006/21:25	006/23:40	LVLH R = 90.0 P = 180.0 Y = 0.0	-YLV/-XVV Sample settling and RCS burn for MEPHISTO operations
006/23:40	007/07:50	LVLH R = 290.92 P = 91.61 Y = 357.95	BIAS -XLV/-YVV Sample settling and RCS burn for MEPHISTO operations
008/02:05	008/06:20	LVLH R = 6.97 P = 184.96 Y = 0.61	BIAS -XLV/+ZVV AADSF stabilization attitude #1
008/06:20	008/06:41		Freedrift
008/06:41	008/11:30	LVLH R = 6.97 P = 184.96 Y = 0.61	BIAS -XLV/+ZVV AADSF stabilization attitude #1
009/02:00	009/11:33	LVLH R = 0.0 P = 90.0 Y = 343.0	BIAS -XLV/+ZVV AADSF stabilization attitude #2
010/02:00	010/11:45	LVLH R = 0.0 P = 123.0 Y = 0.0	BIAS -XLV/+ZVV AADSF stabilization attitude #3
010/11:45	010/12:30	LVLH R = 90.0 P = 180.0 Y = 0.0	-YLV/-XVV Sample settling, RCS burn for MEPHISTO operations
010/12:30	010/12:40		Freedrift
010/12:40	010/14:00	LVLH R = 90.0 P = 180.0 Y = 0.0	-YLV/-XVV Sample settling, MEPHISTO operations
012/12:25	012/12:40	LVLH Hold R = 359.56 P = 95.02 Y = 4.98	Freedrift and PRCS (-Z 15 sec.)
012/14:25	012/14:28	LVLH Hold R = 359.56 P = 95.02 Y = 4.98	Freedrift and PRCS (+Y 15 sec.)

Table 10. Subset of STS-75 As-flown Attitude Timeline (cont.)

012/14:28	012/15:45	LVLH Hold R = 359.56 P = 95.02 Y = 4.98	Freedrift and PRCS (-Y 15 sec.)
012/15:45	012/16:34	various	MEPHISTO rotational maneuvers
012/16:34	012/16:48		Freedrift
013/12:05	013/12:50	LVLH R = 290.92 P = 91.61 Y = 357.95	BIAS -XLV/-YVV MEPHISTO gravity gradient
013/12:50	013/13:00	LVLH Hold R = 290.92 P = 91.61 Y = 357.95	Freedrift and PRCS (+Z 15 sec)
013/13:00	013/13:20	LVLH Hold R = 290.92 P = 91.61 Y = 357.95	MEPHISTO gravity gradient
013/13:20	013/14:03	LVLH R = 166.06 P = 338.90 Y = 319.97	-ZLV/+XVV MEPHISTO attitude for OMS burn
013/14:03			MEPHISTO OMS burn (2 engines, 30 seconds)
013/14:03	013/14:30		Freedrift
013/14:30	Landing		Orbiter operations

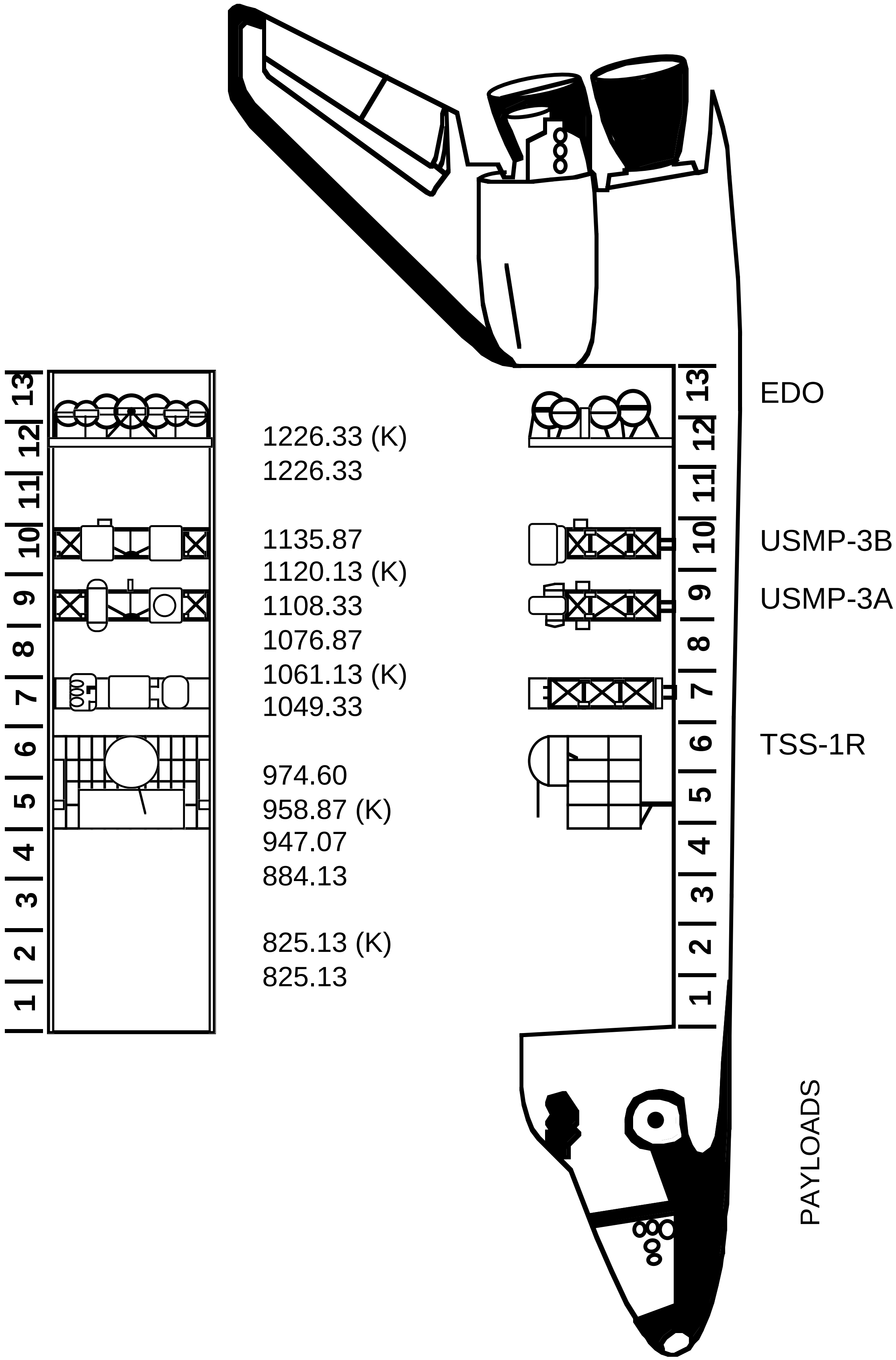

Fig. 1 Cargo bay configuration for STS-75

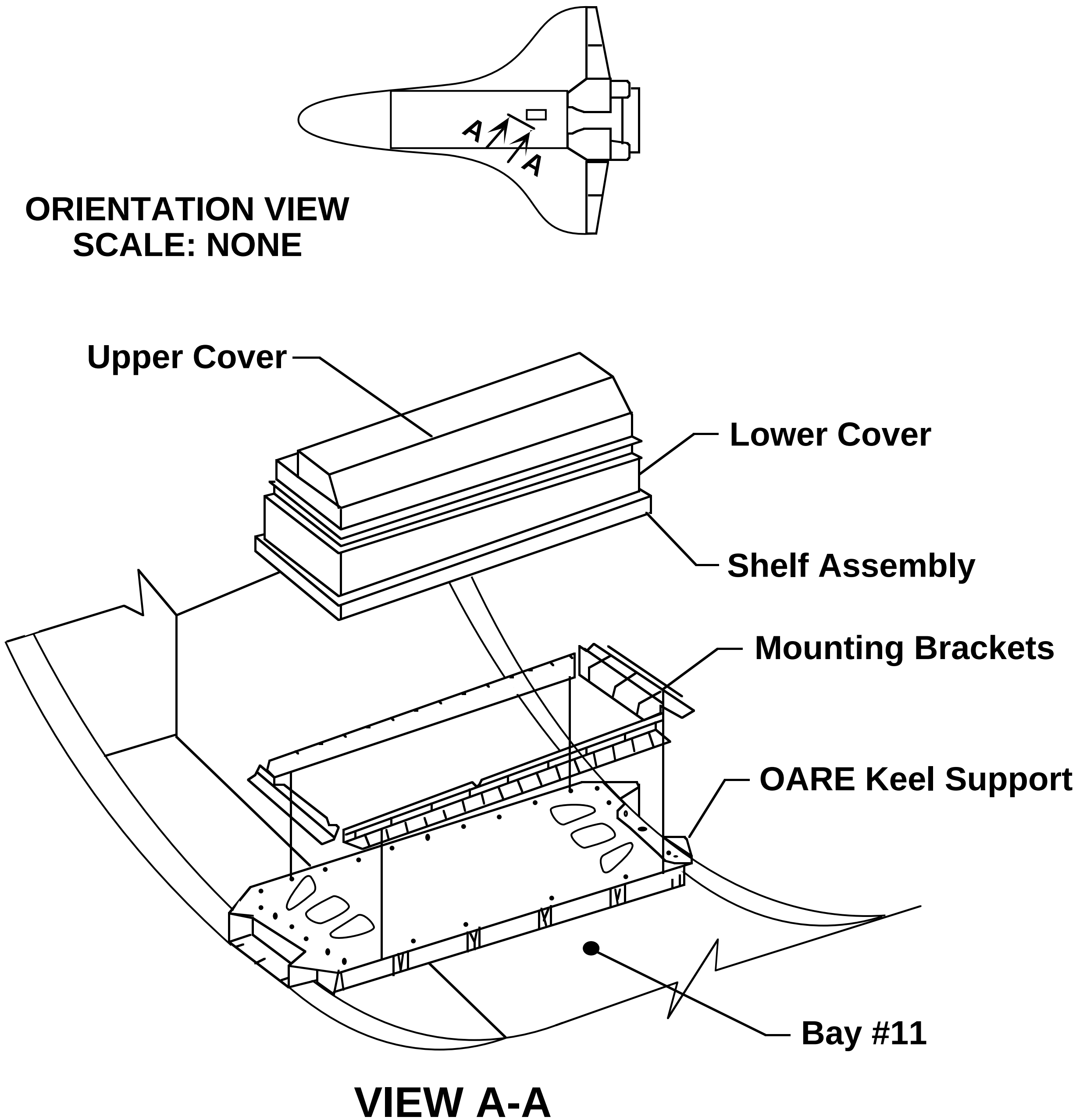

Fig. 2 OARE instrument location on STS-75

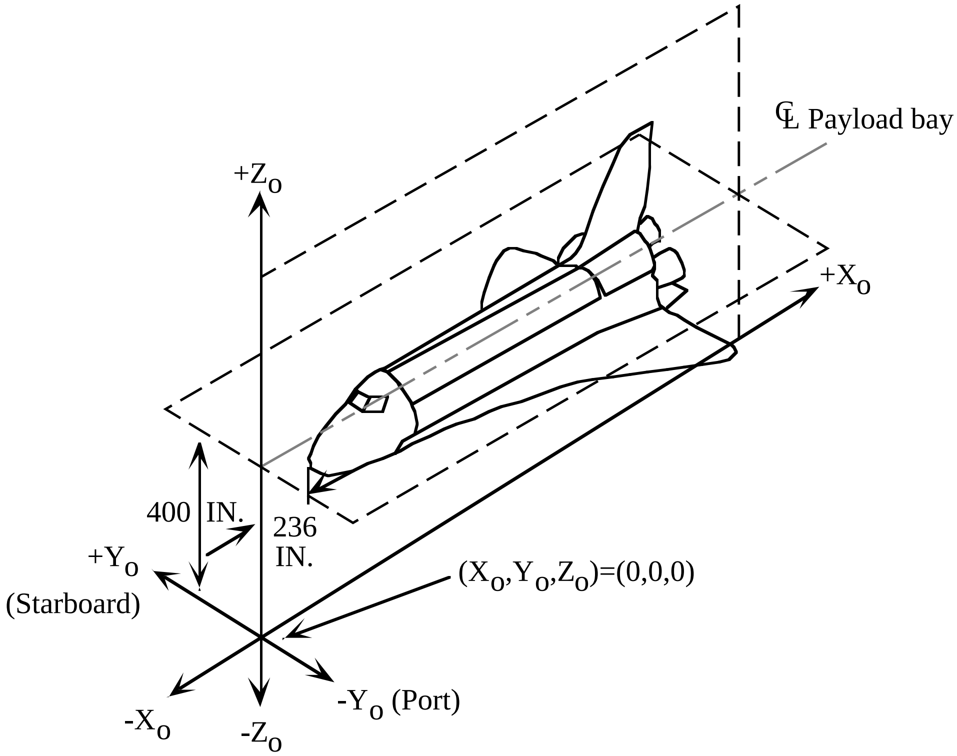

Orbiter structural coordinate system.

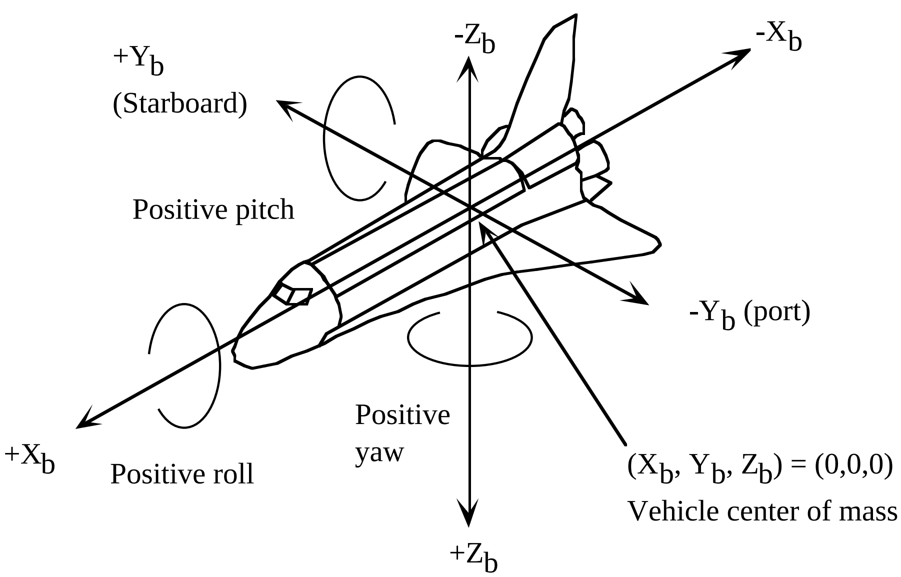

Orbiter body coordinate system.

Fig. 3 Orbiter body and structural coordinate systems

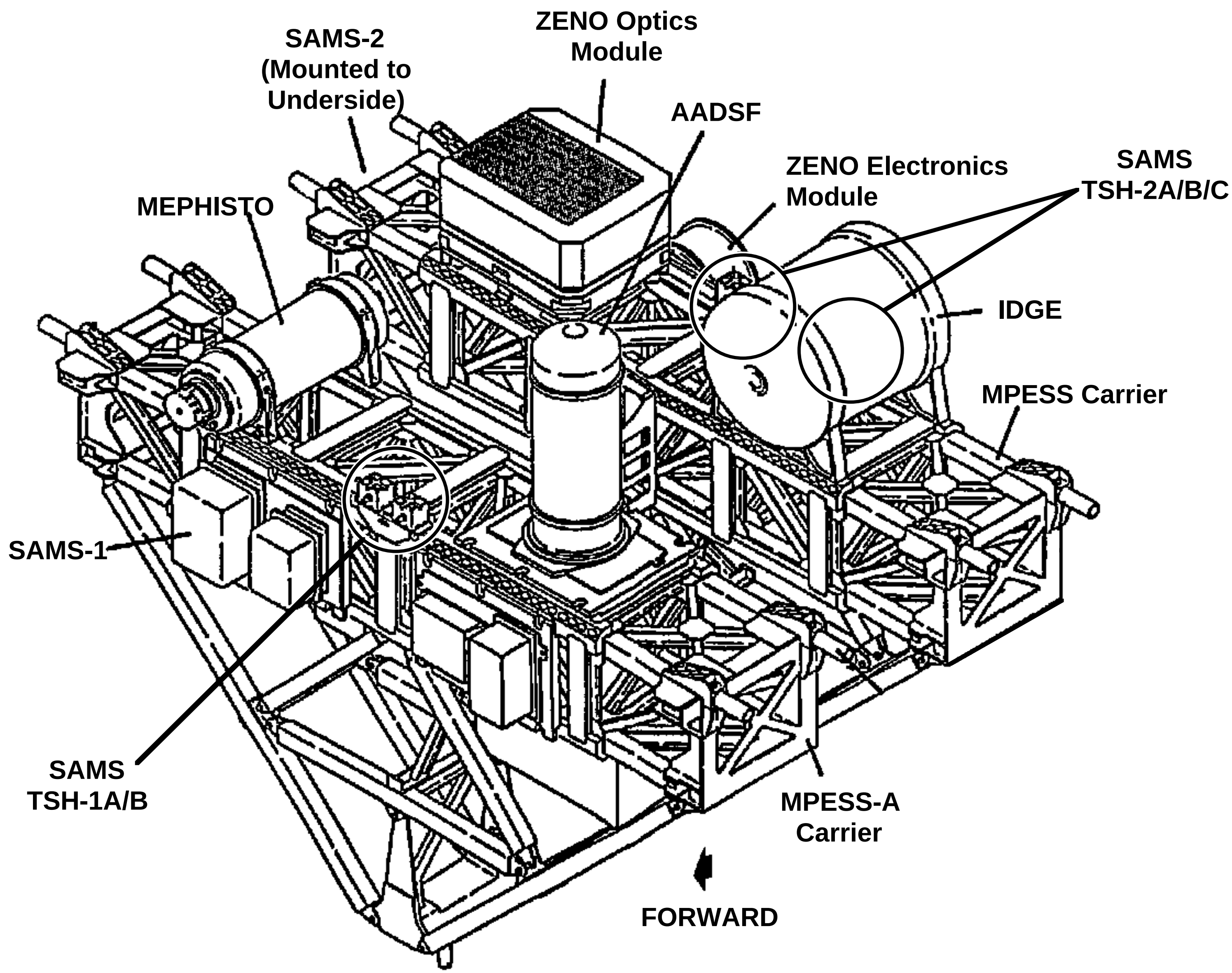

Fig. 4 Approximate location of SAMS sensors on the USMP-3 MPESS carriers, STS-75

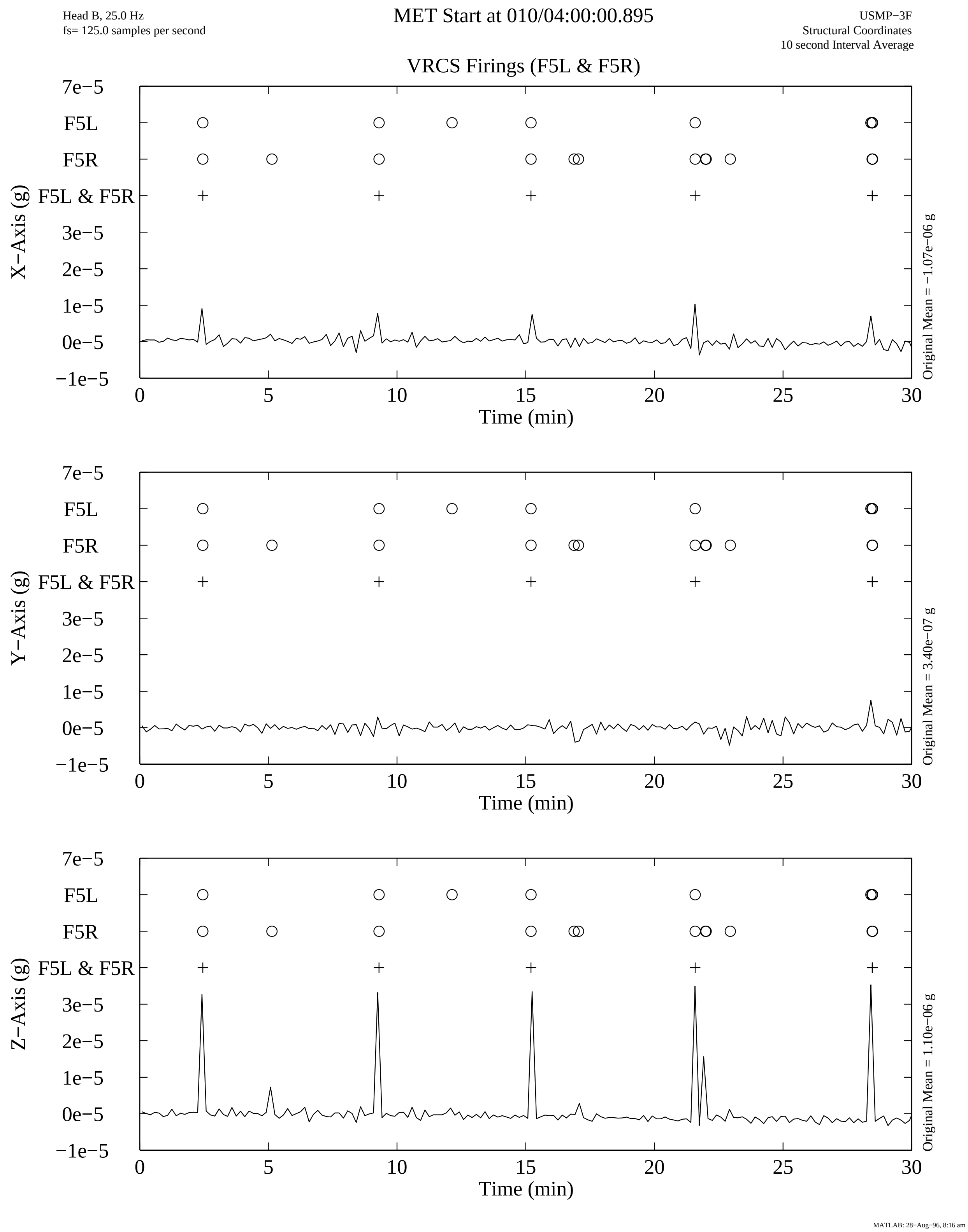

Fig. 5 SAMS Unit F TSH 1B data, ten second interval average, showing use of F5L and F5R VRCS jets for attitude maintenance. Simultaneous F5L and F5R jet firings indicated by + markers, individual events indicated by o markers. MET start 010/04:00.

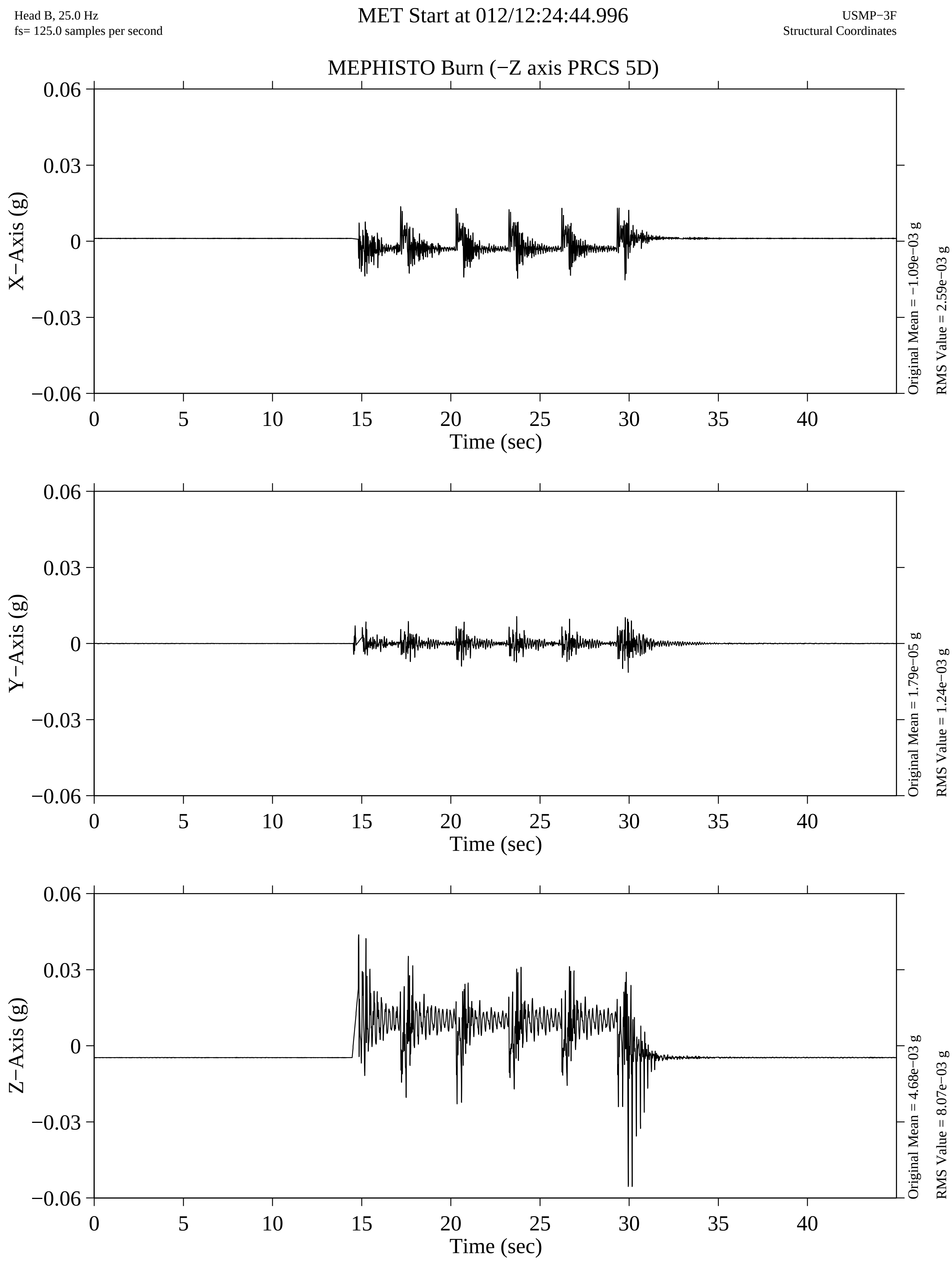

Fig. 6 SAMS Unit F TSH 1B data from MEPHISTO PRCS 5D (-Z_b) event. MET start 012/12:24:45.

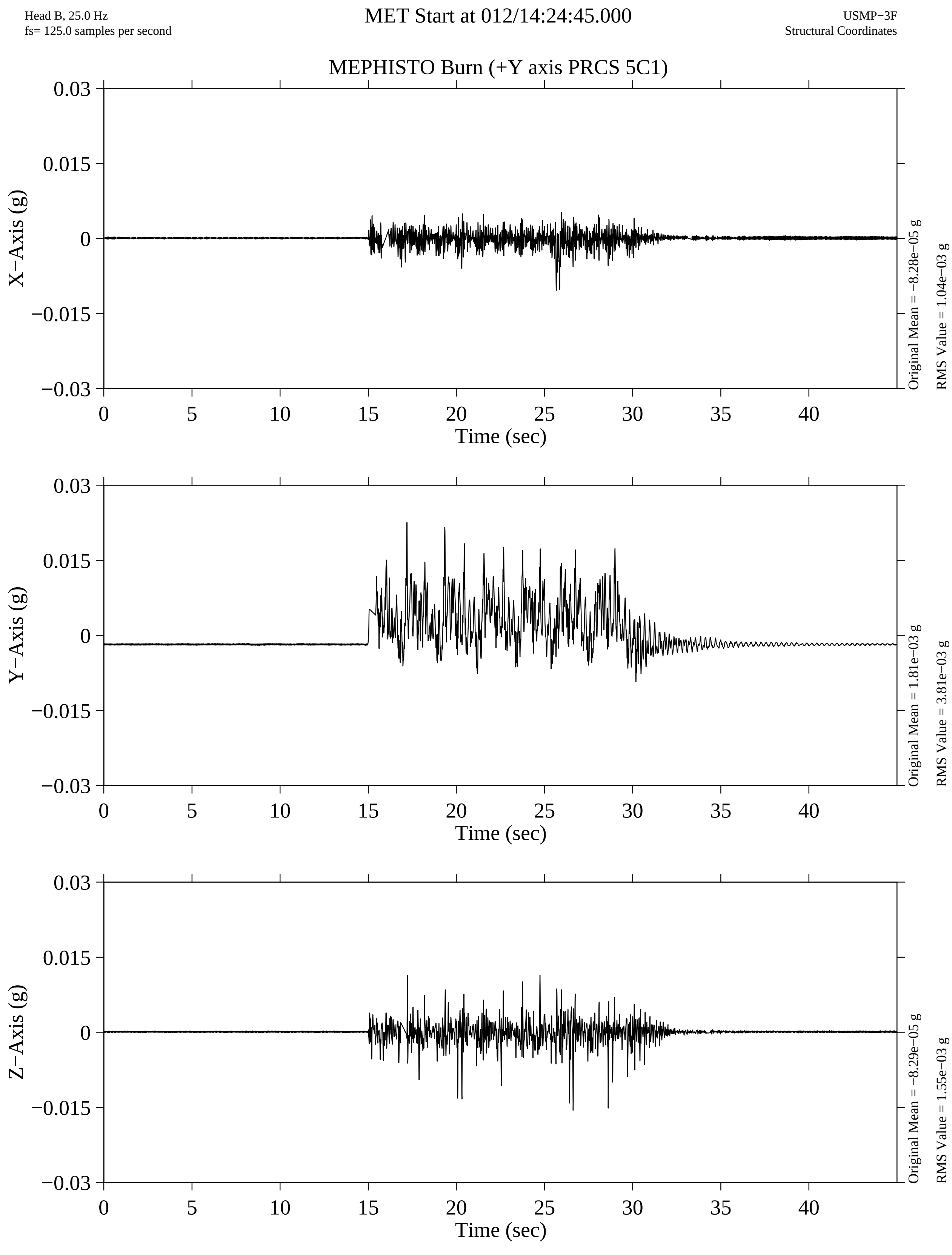

Fig. 7 SAMS Unit F TSH 1B data from MEPHISTO PRCS 5C1 (+Y_b) event. MET start 012/14:24:45

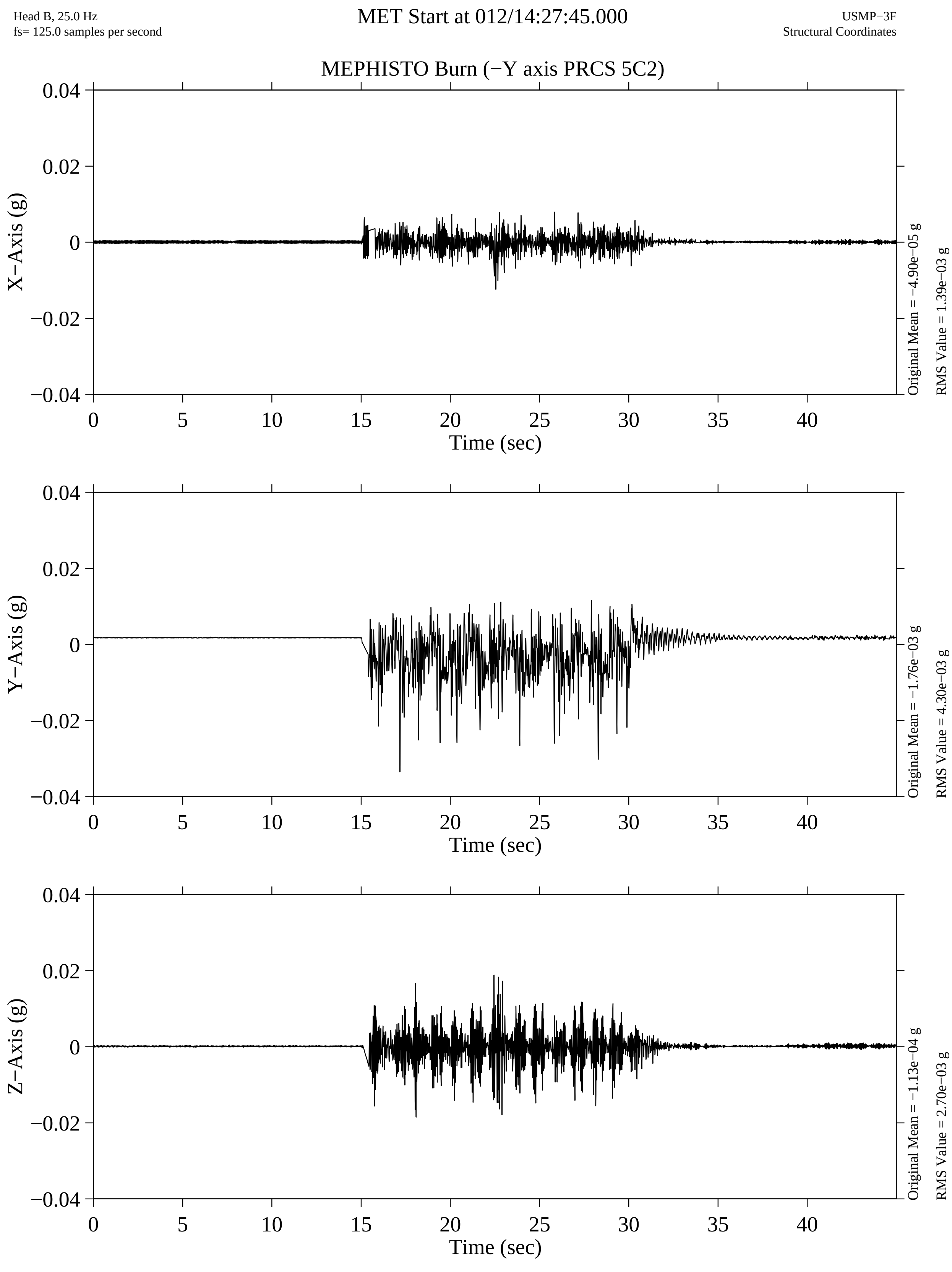

Fig. 8 SAMS Unit F TSH 1B data from MEPHISTO PRCS 5C2 (-Y_b) event. MET start 012/14:27:45.

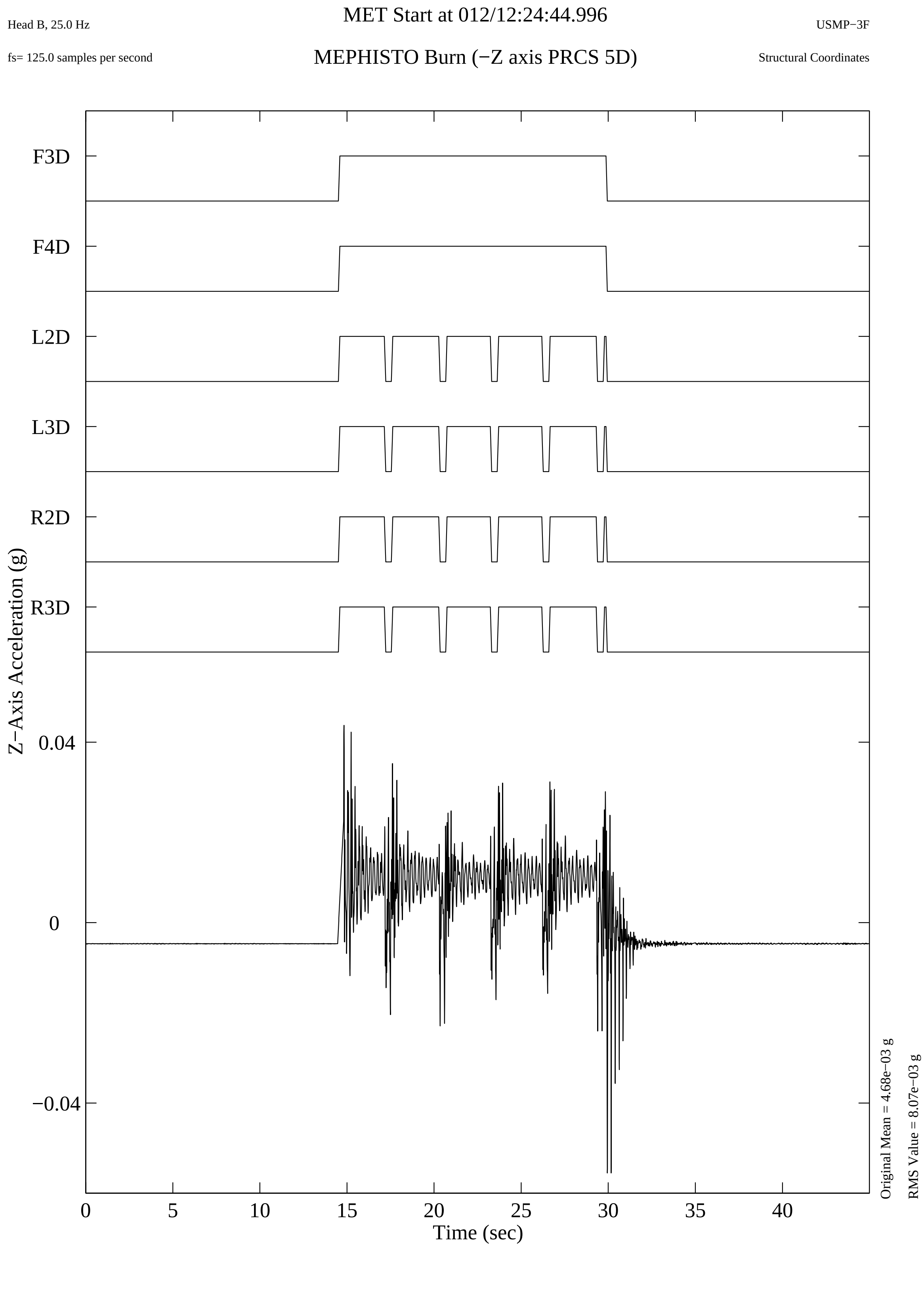

Fig. 9 SAMS Unit F TSH 1B data from MEPHISTO PRCS 5D (-Z_b) event, Z_O axis of data shown. PRCS jet usage indicate on top section of plot. MET start 012/12:24:45

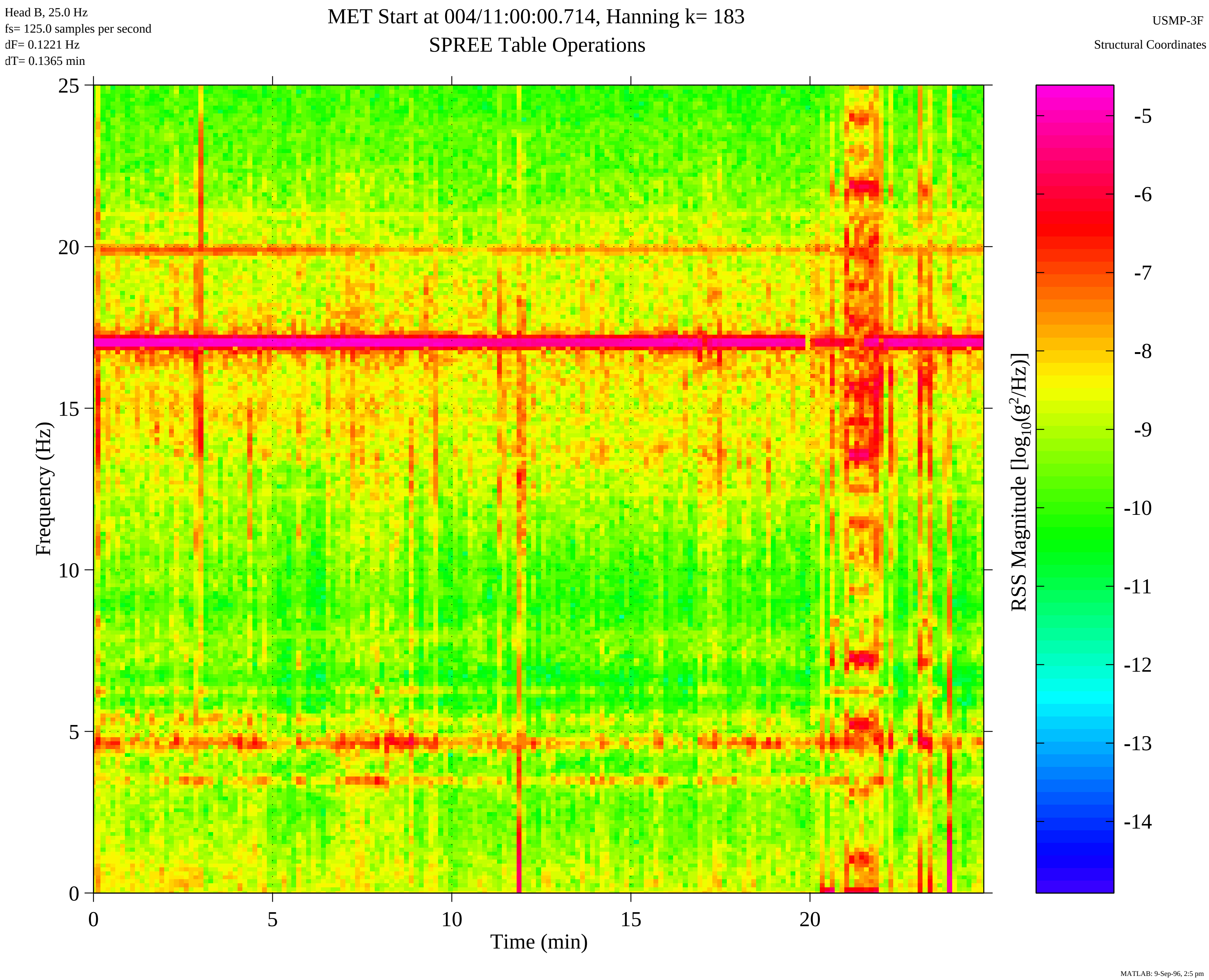

Fig. 10 SAMS Unit F TSH 1B spectrogram showing data collected during SPREE Table Rotation Operations. MET start 004/11:00.

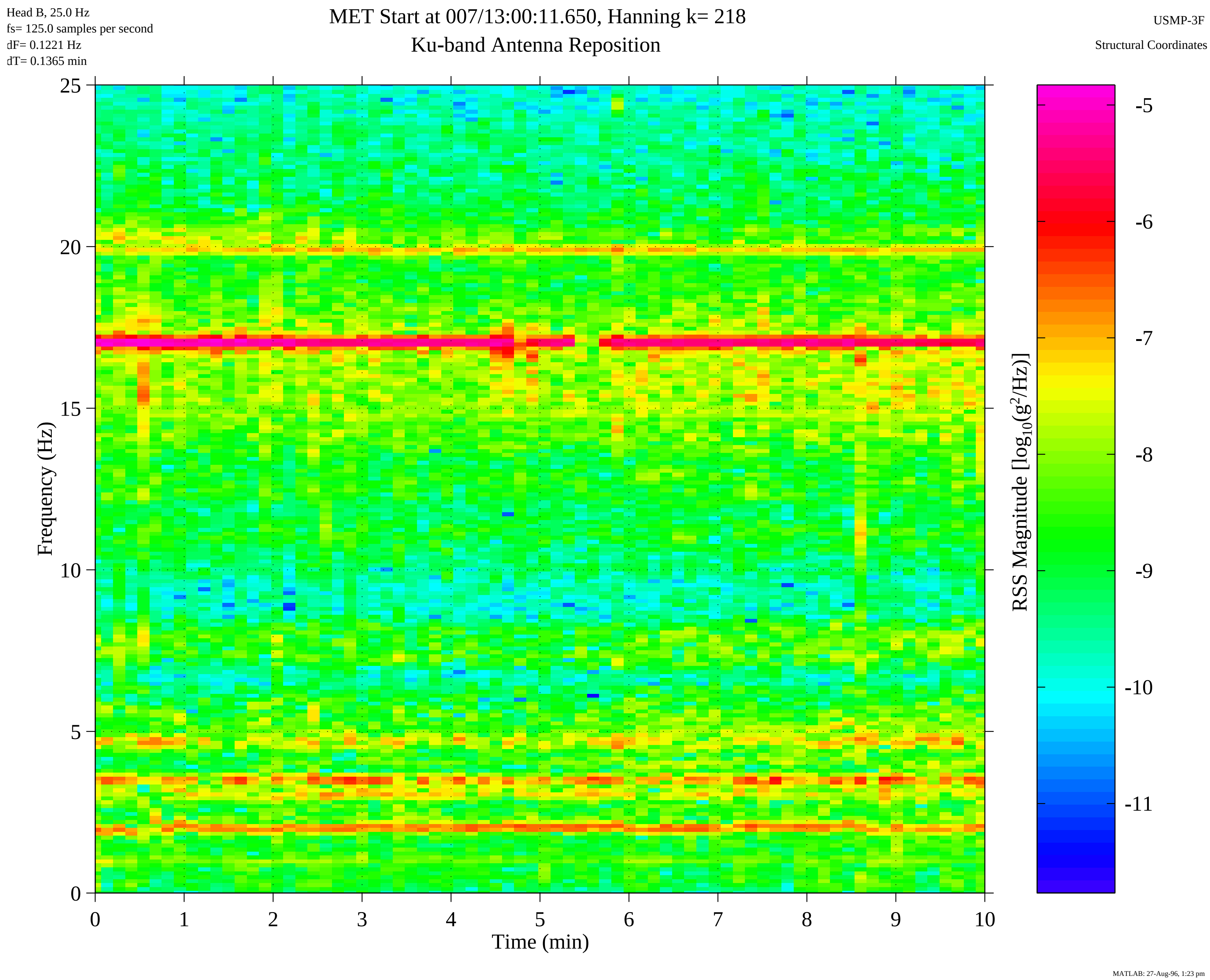

Fig. 11 SAMS Unit F TSH 1B spectrogram showing data collected during Ku band antenna reposition. MET start 007/13:00:12. Note interruption of 17 Hz signal at 007/13:05:25 for 17 seconds.

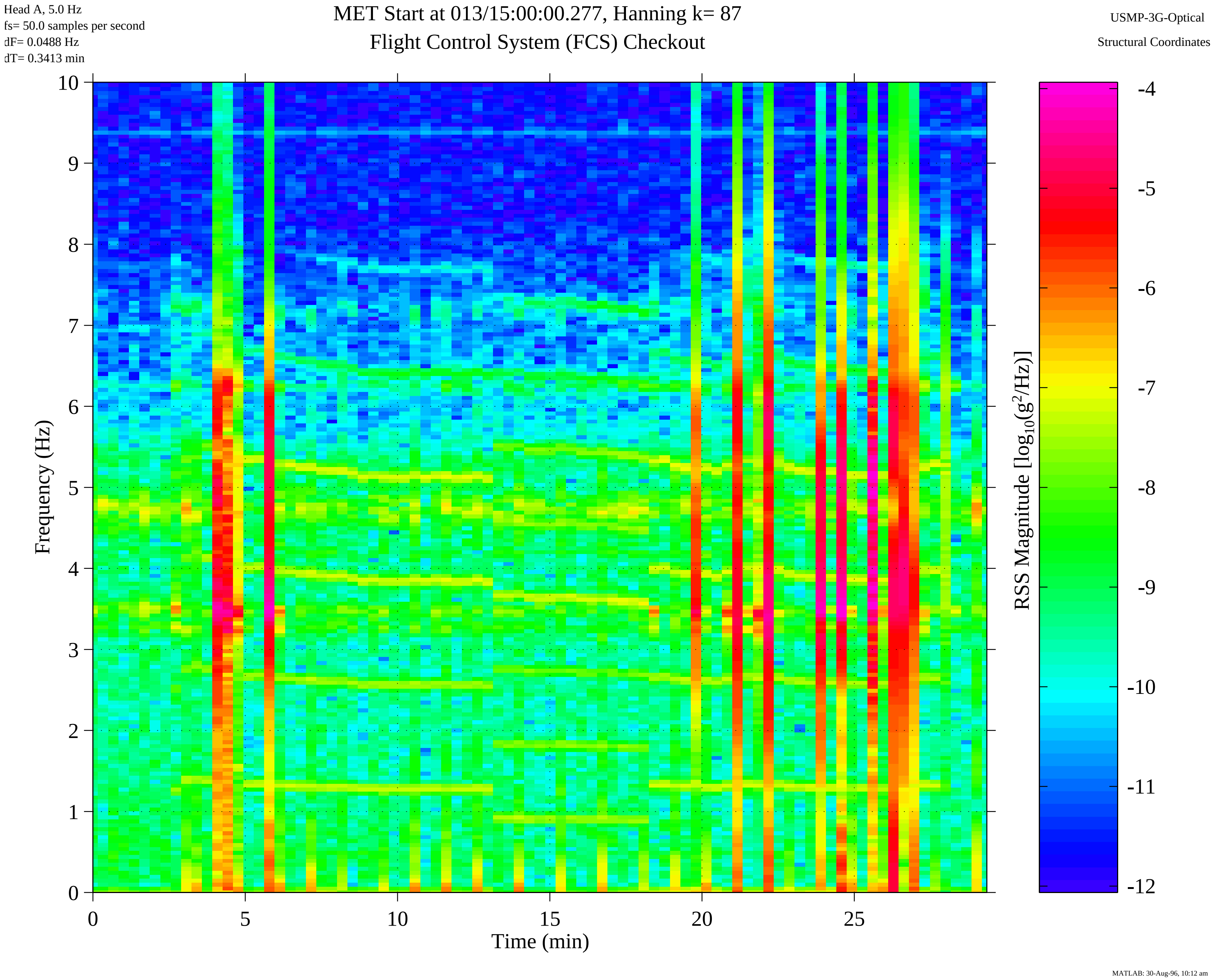

Fig. 12 SAMS Unit G TSH 2A spectrogram showing data collected during Flight Control System checkout. MET start 013/15:00:00. Note change in signal character upon activation of auxiliary power unit one at 013/15:03.

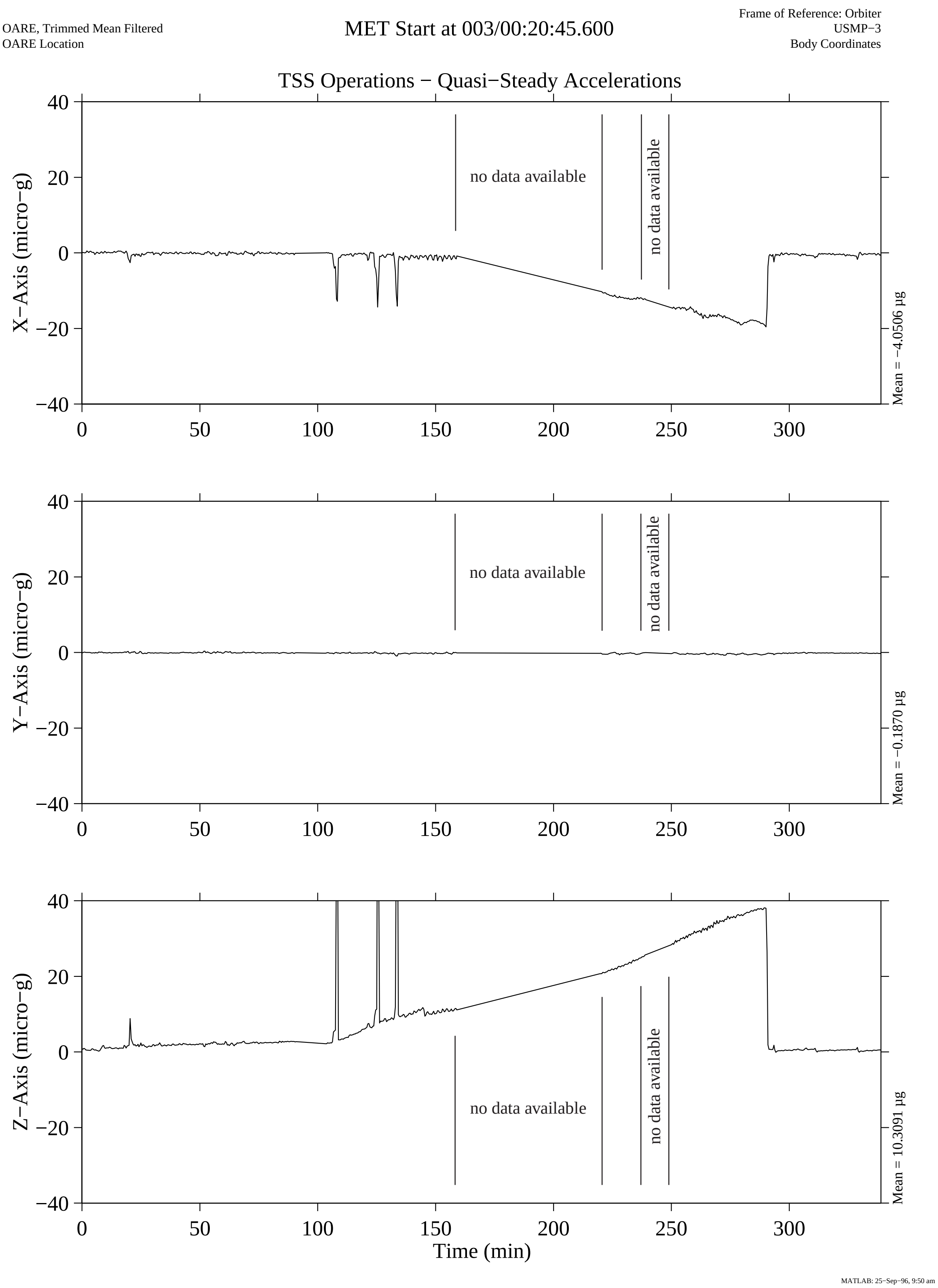

Fig. 13 OARE data representing the microgravity environment at the OARE location during TSS-1R deploy operations. MET start at 003/00:00. Note TSS flyaway occurred at 003/00:27. Transient accelerations seen in the plot are due to PRCS activity to compensate for tether dynamics.

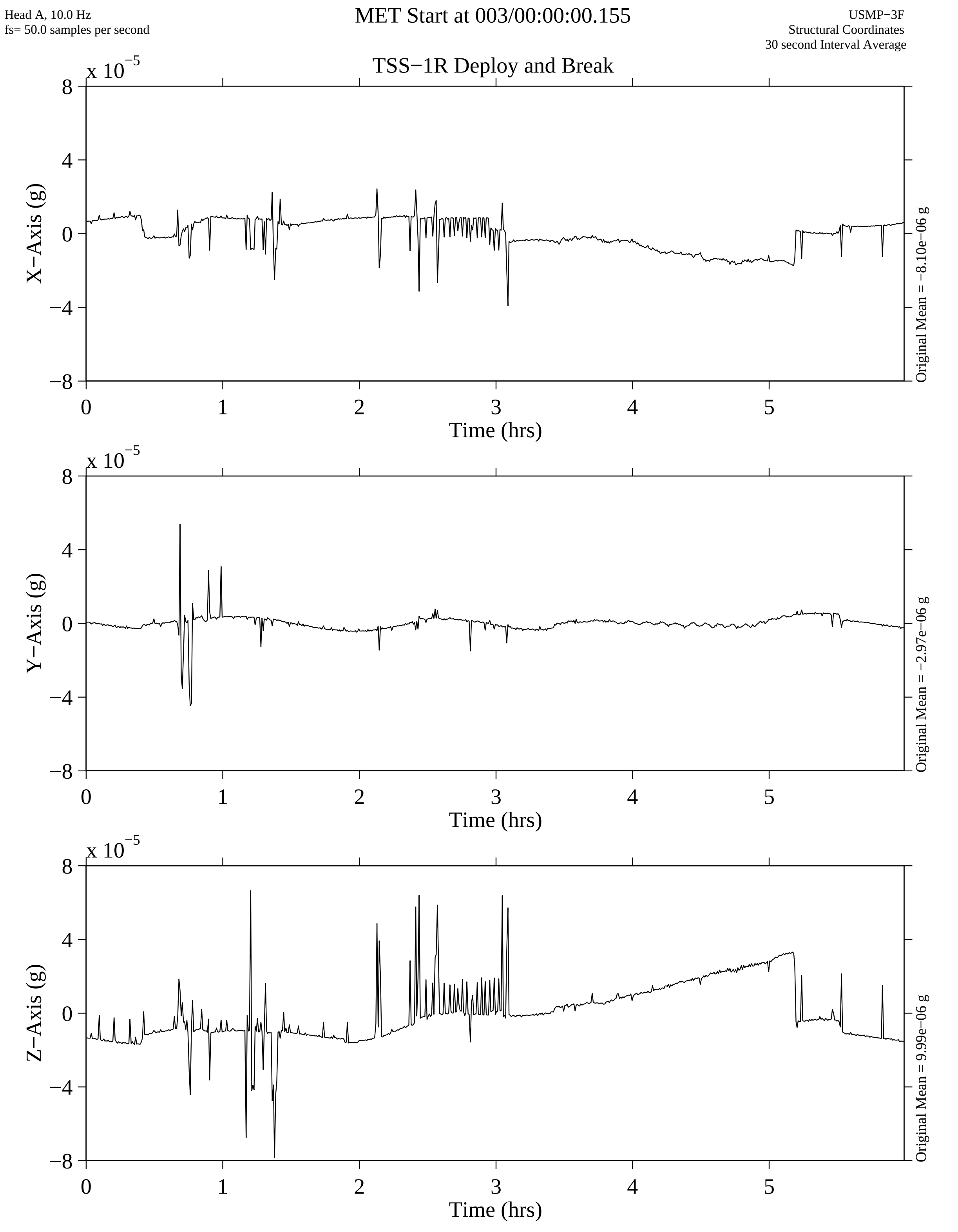

Fig. 14 SAMS Unit F TSH 1A data representing the microgravity environment during TSS-1R deploy operations. MET start at 003/00:00. Note TSS flyaway occurred at 003/00:27. Transient accelerations seen in the plot are due to PRCS activity to compensate for tether dynamics.

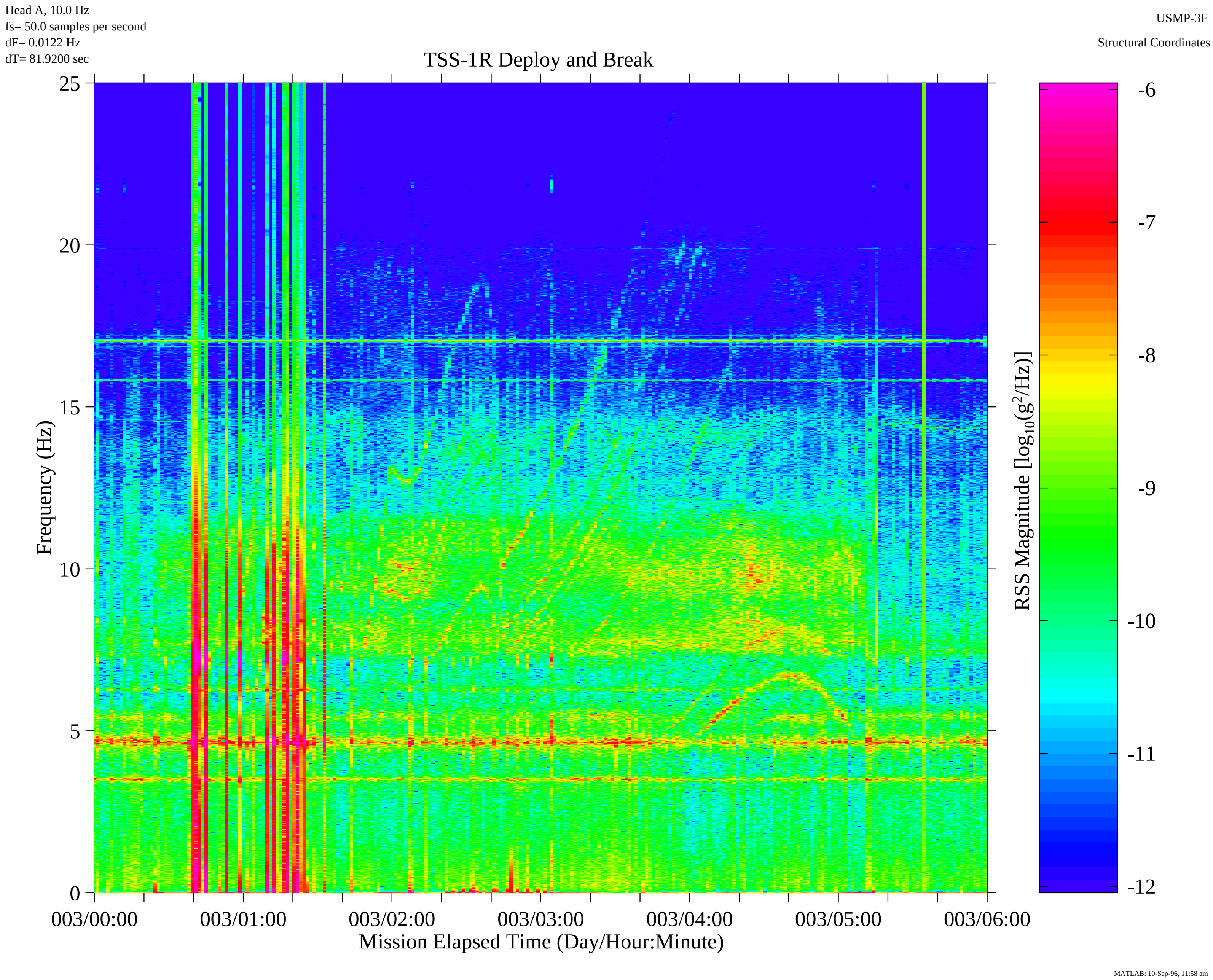

Fig. 15 SAMS Unit F TSH 1A spectrogram showing data collected during TSS-1R deploy operations. MET start at 003/00:00. Note TSS flyaway occurred at 003/00:27. Transient accelerations seen in the plot as vertical stripes are due to PRCS activity to compensate for tether dynamics. Variable frequency traces are related to tether pulley rotations during tether deploy.

THIS PAGE IS TEMPORARLIY NOT AVAILABLE

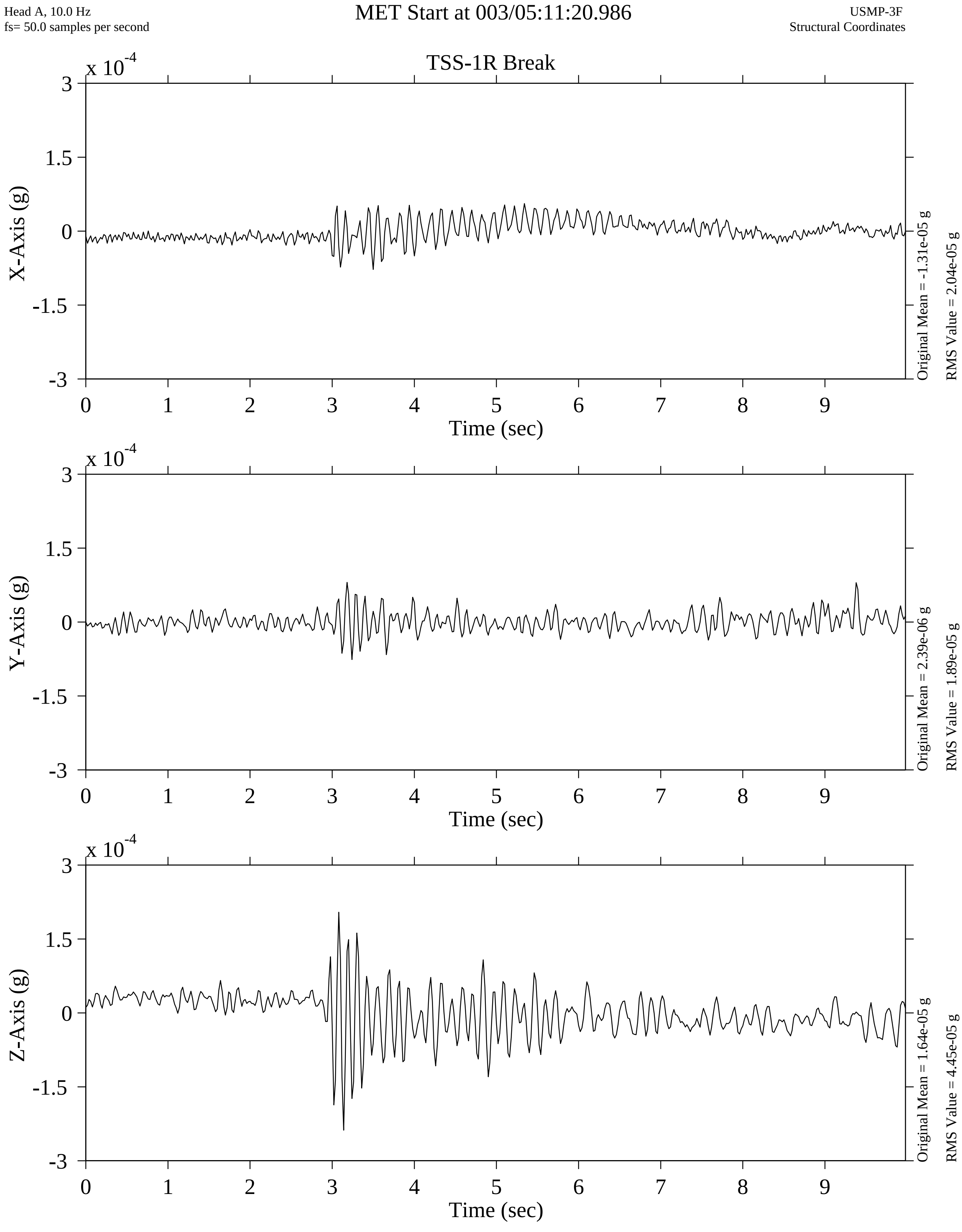

Fig. 17 SAMS Unit F TSH 1A data from time of TSS-1R break. Note ringing of Orbiter structure at about 9 Hz.

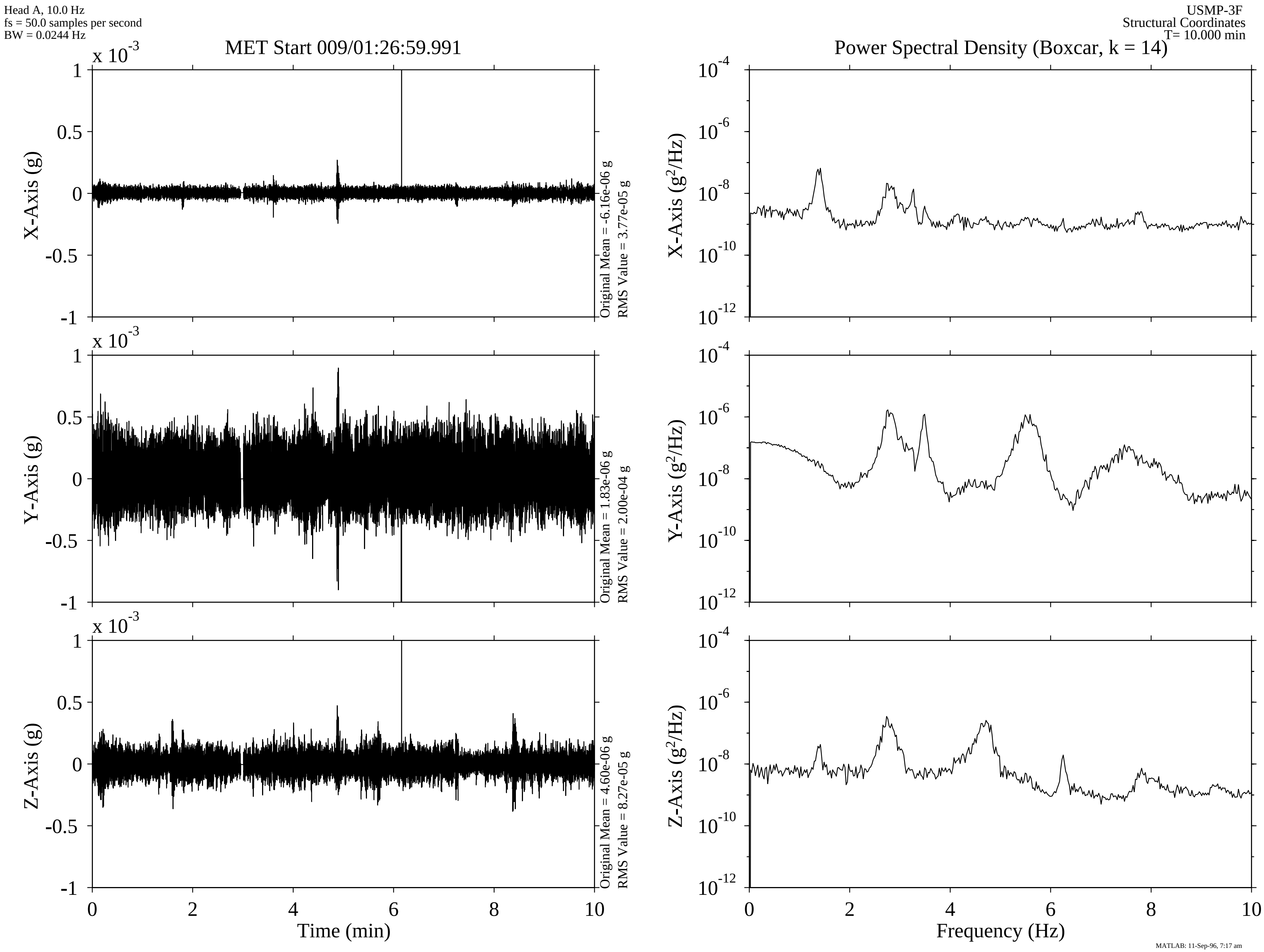

Fig. 18 SAMS Unit F TSH 1A data from Waste Collection System compaction operations. No disturbances associated with this operation appear in the data.

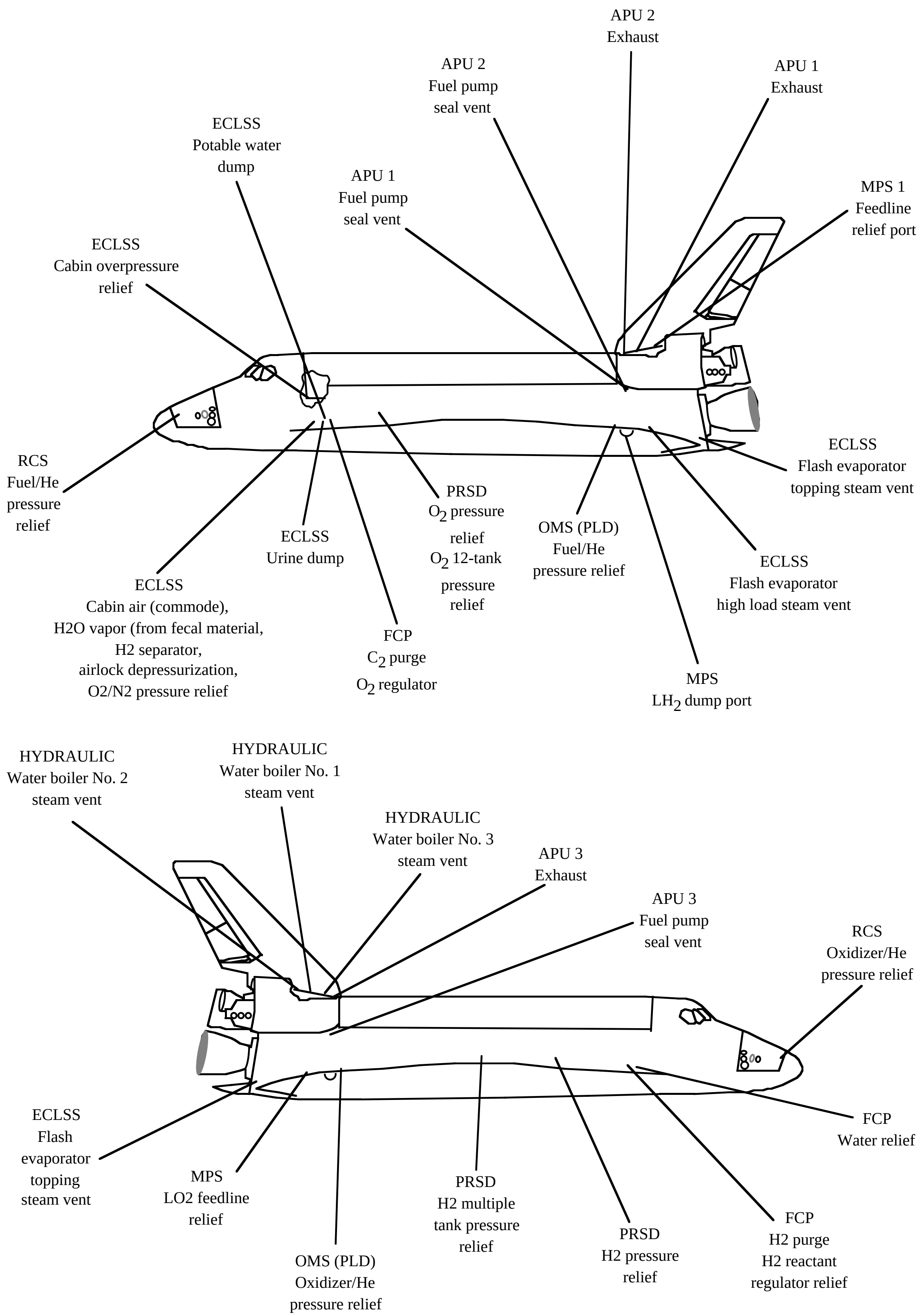

Fig. 19 Orbiter venting locations [13].

THIS PAGE IS TEMPORARLIY NOT AVAILABLE

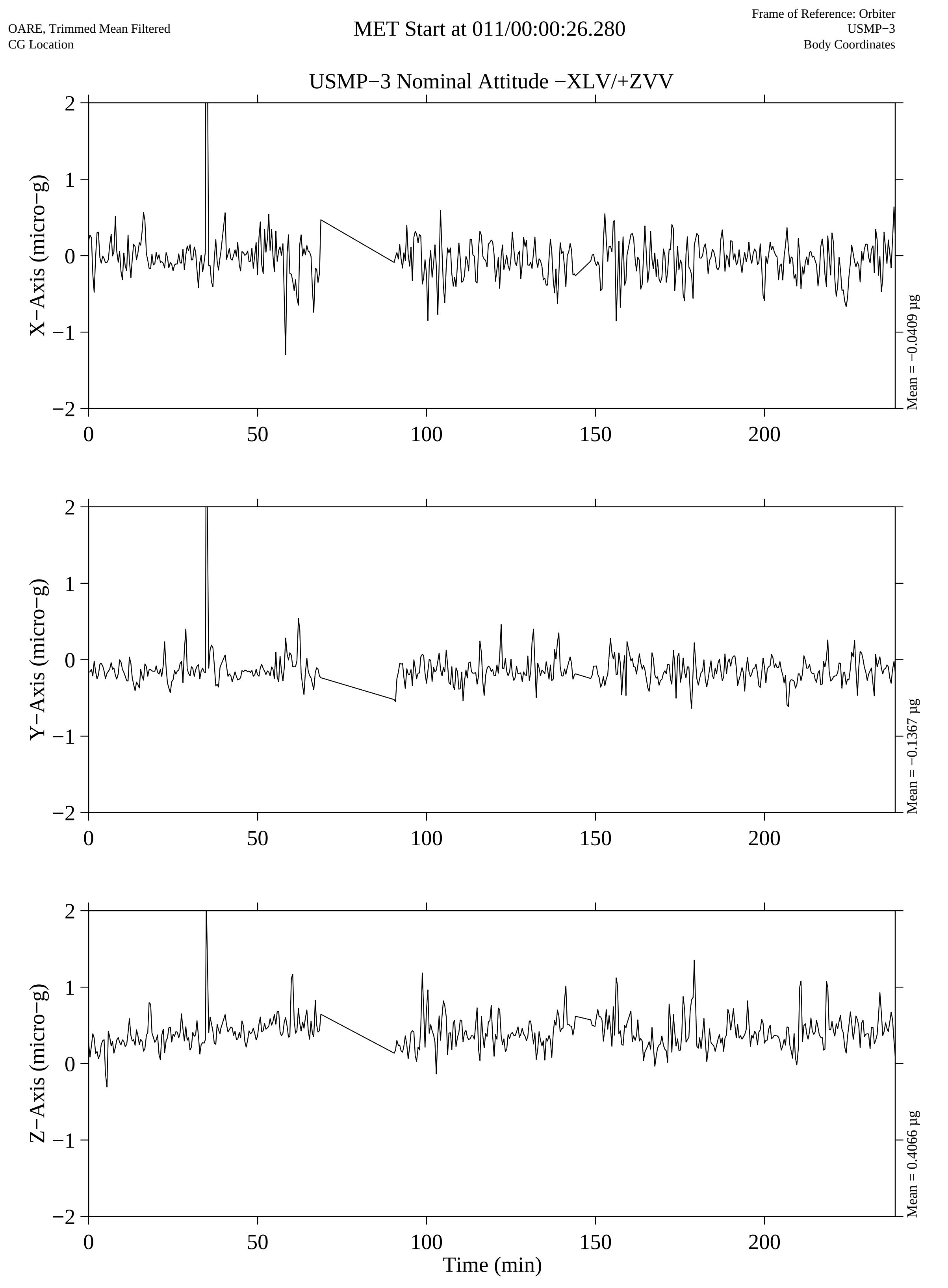

Fig. 21 OARE data representing the microgravity environment at the OARE location while Columbia was in the nominal USMP-3 attitude. MET start at 011/00:00:26.

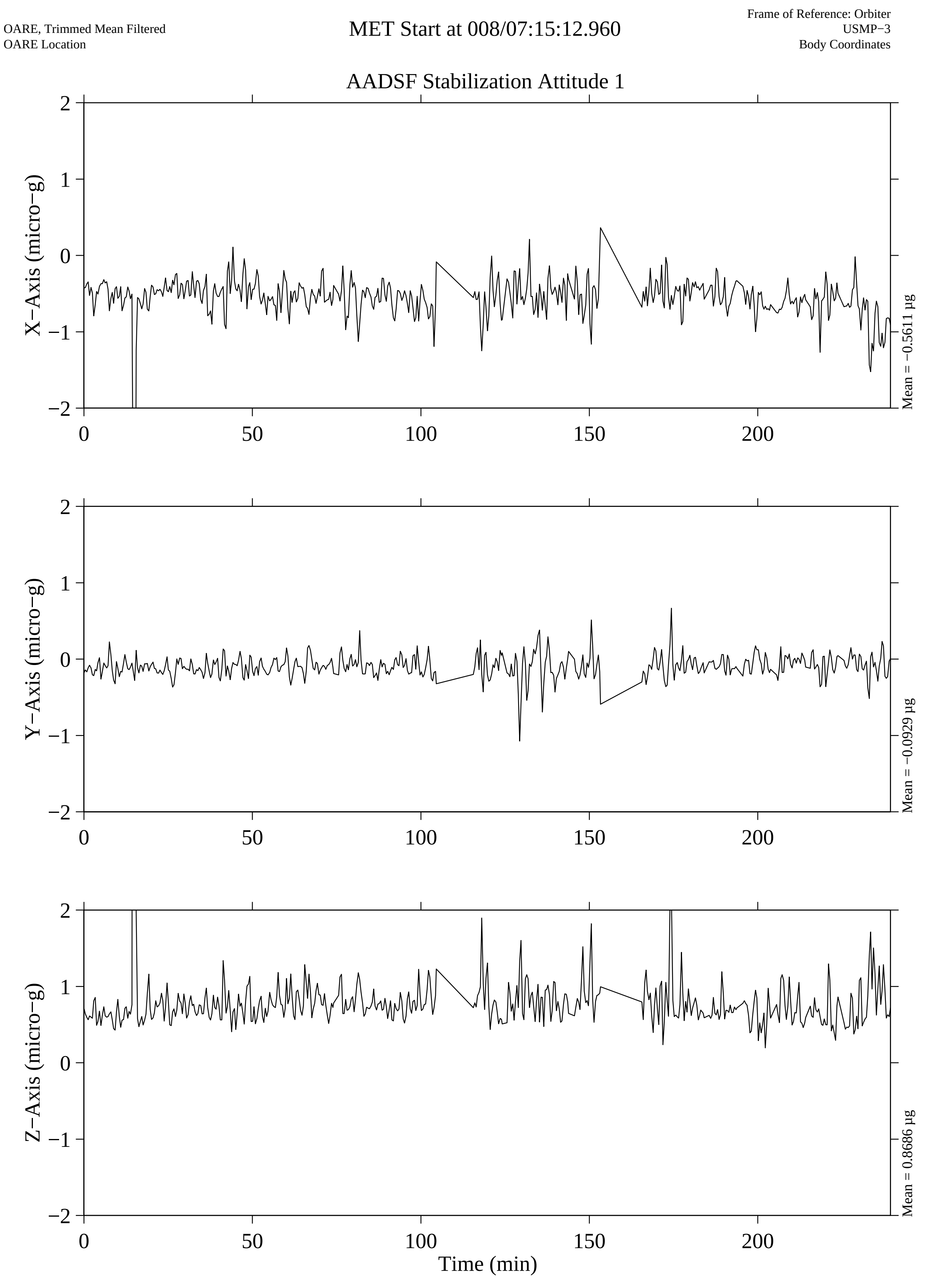

Fig. 22 OARE data representing the microgravity environment at the OARE location while Columbia was in the AADSF 1 attitude. MET start at 008/07:15:13.

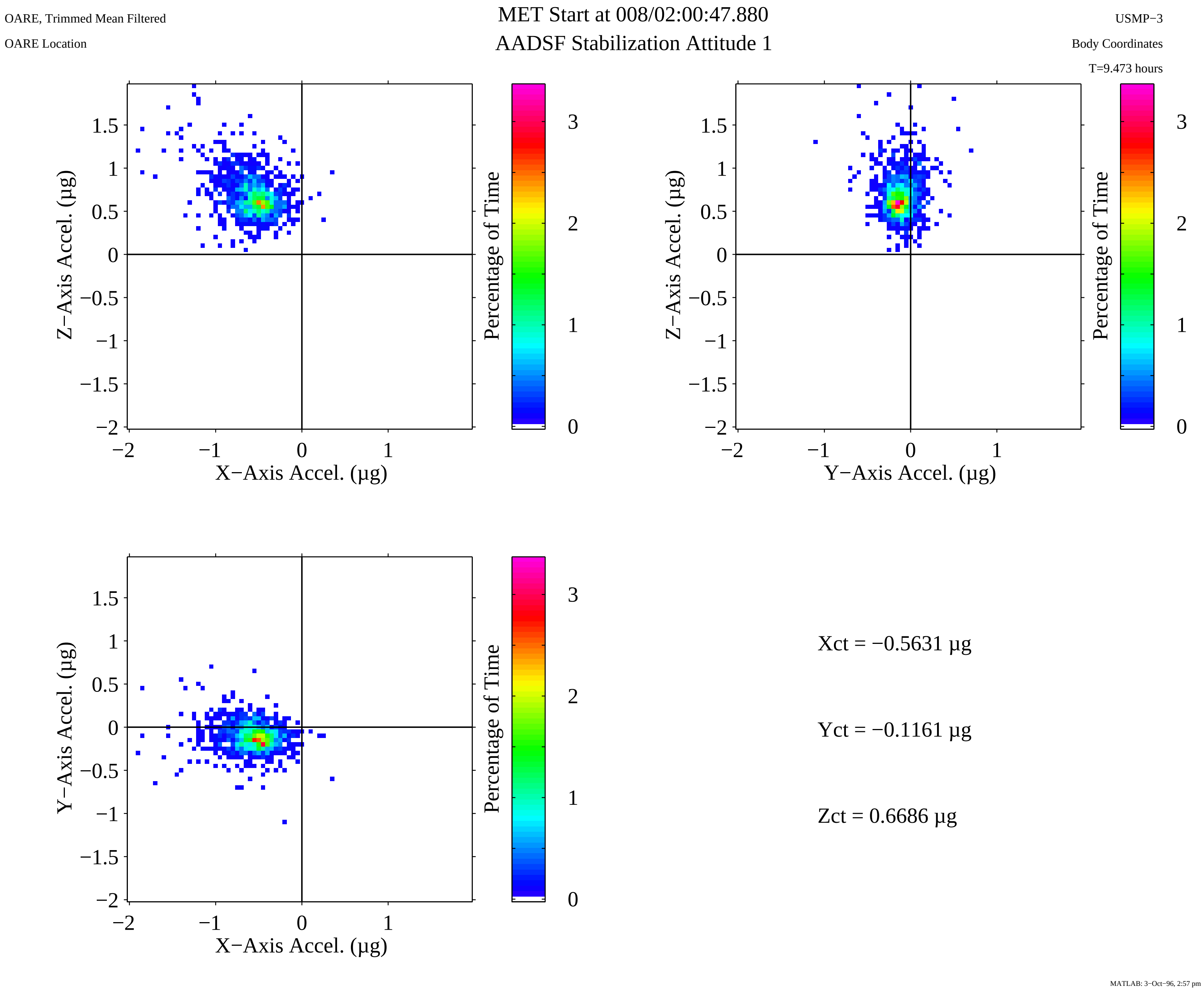

Fig. 23 Three-dimensional projection of OARE data representing the microgravity environment at the OARE location while Columbia was in the AADSF 1 attitude. MET start at 008/02:00:47.

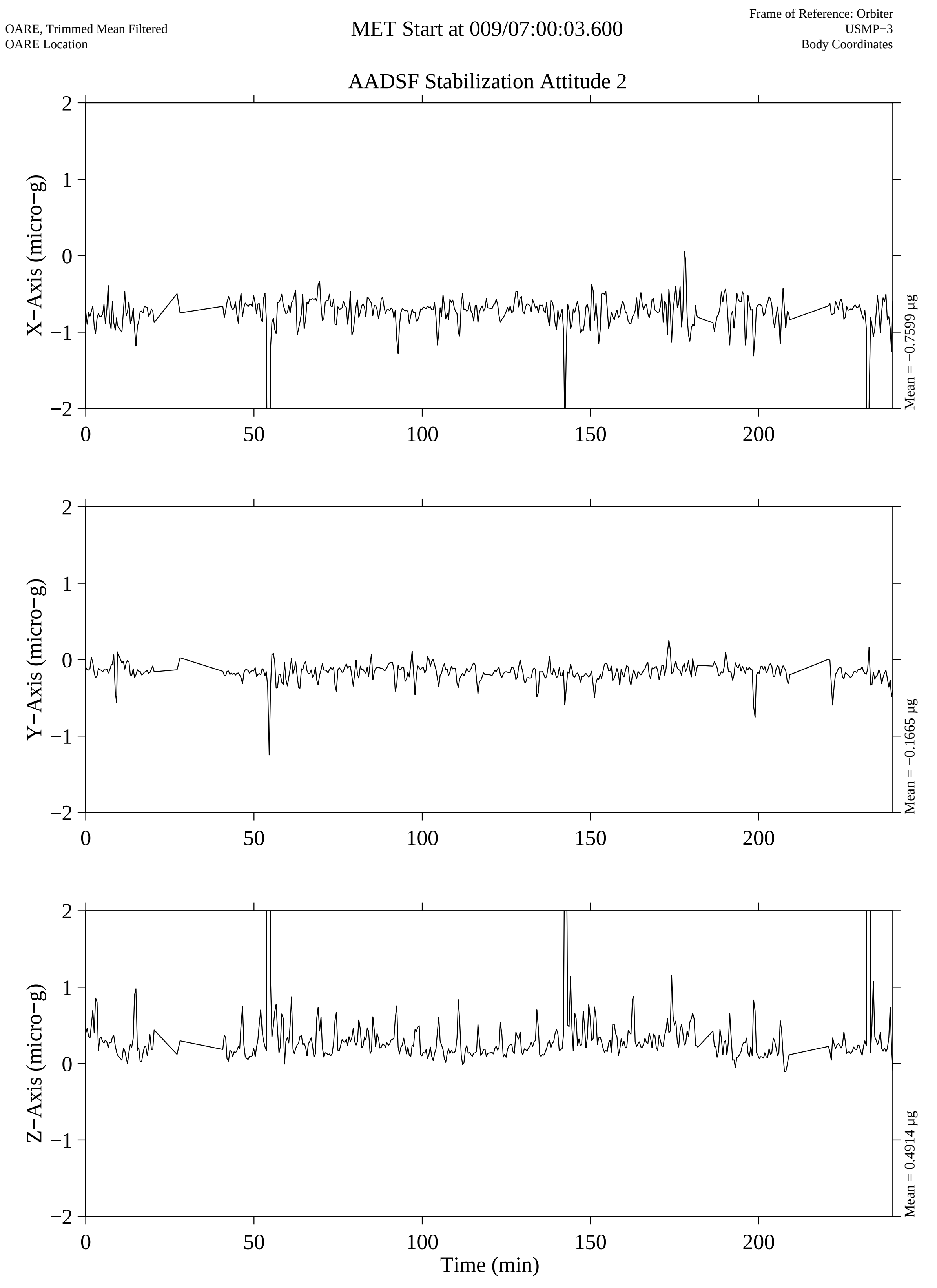

Fig. 24 OARE data representing the microgravity environment at the OARE location while Columbia was in the AADSF 2 attitude. MET start at 009/07:00:03.

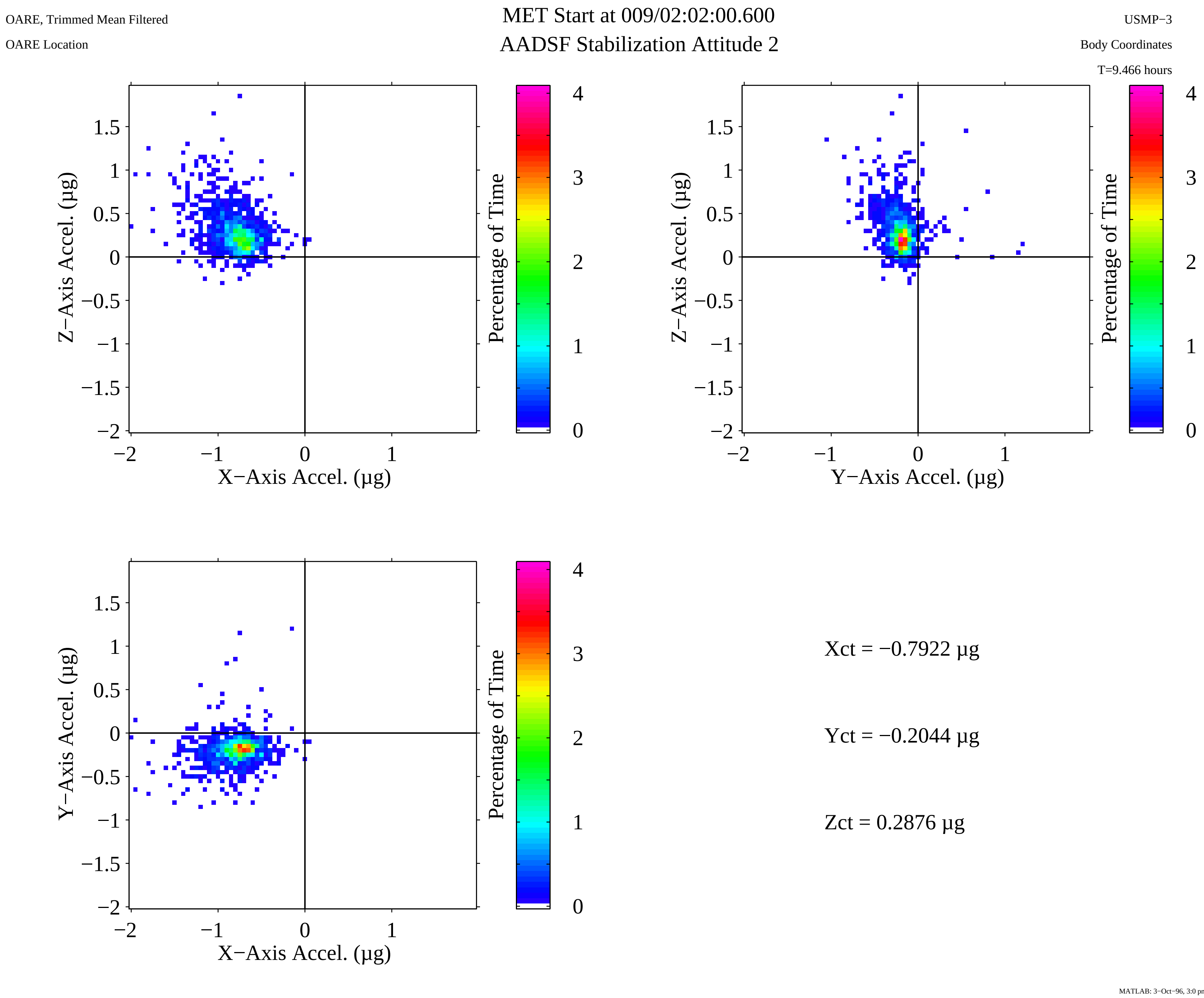

Fig. 25 Three-dimensional projection of the OARE data representing the microgravity environment at the OARE location while Columbia was in the AADSF 2 attitude. MET start at 009/02:02:00.

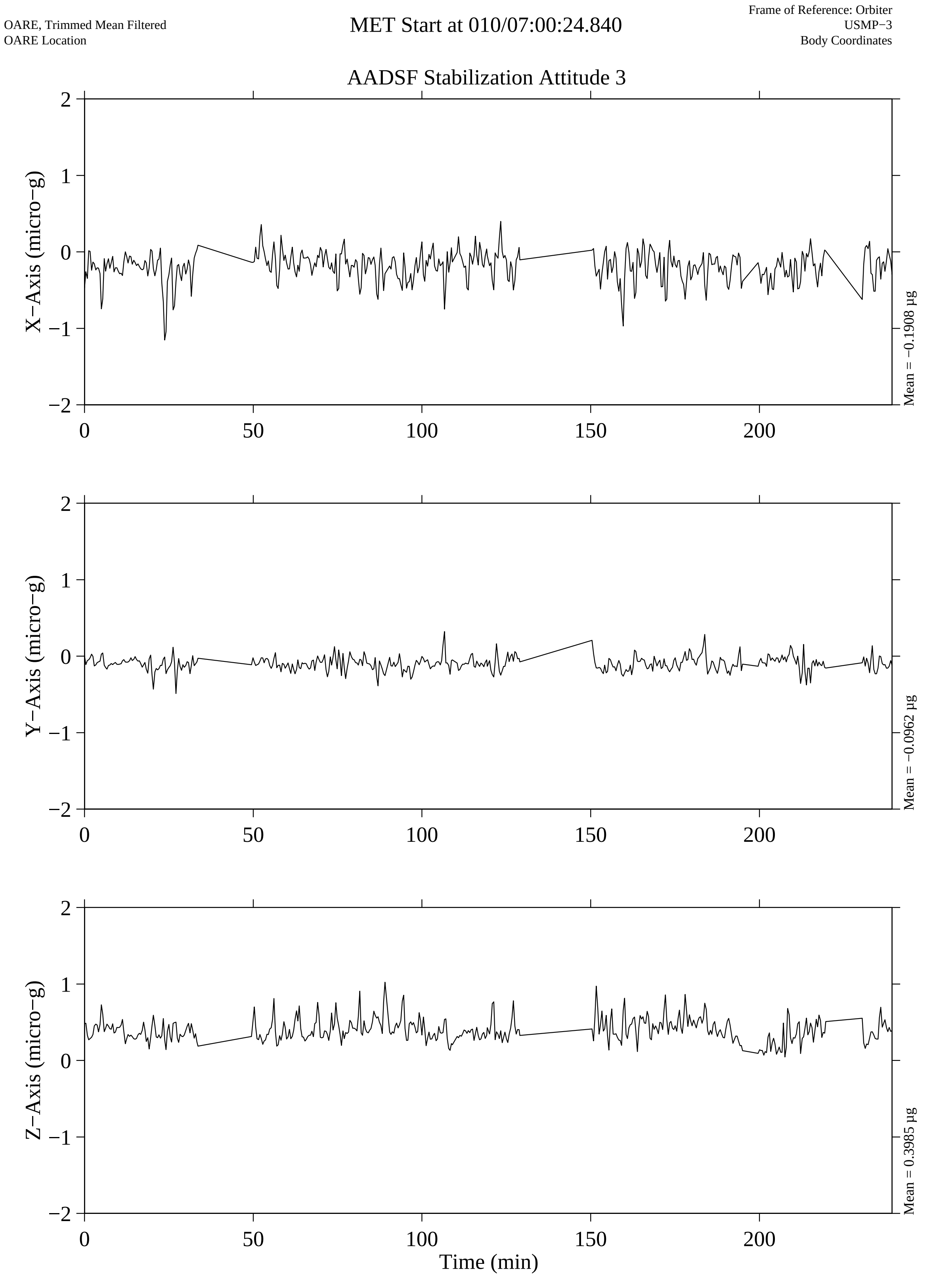

Fig. 26 OARE data representing the microgravity environment at the OARE location while Columbia was in the AADSF 3 attitude. MET start at 010/07:00:24.

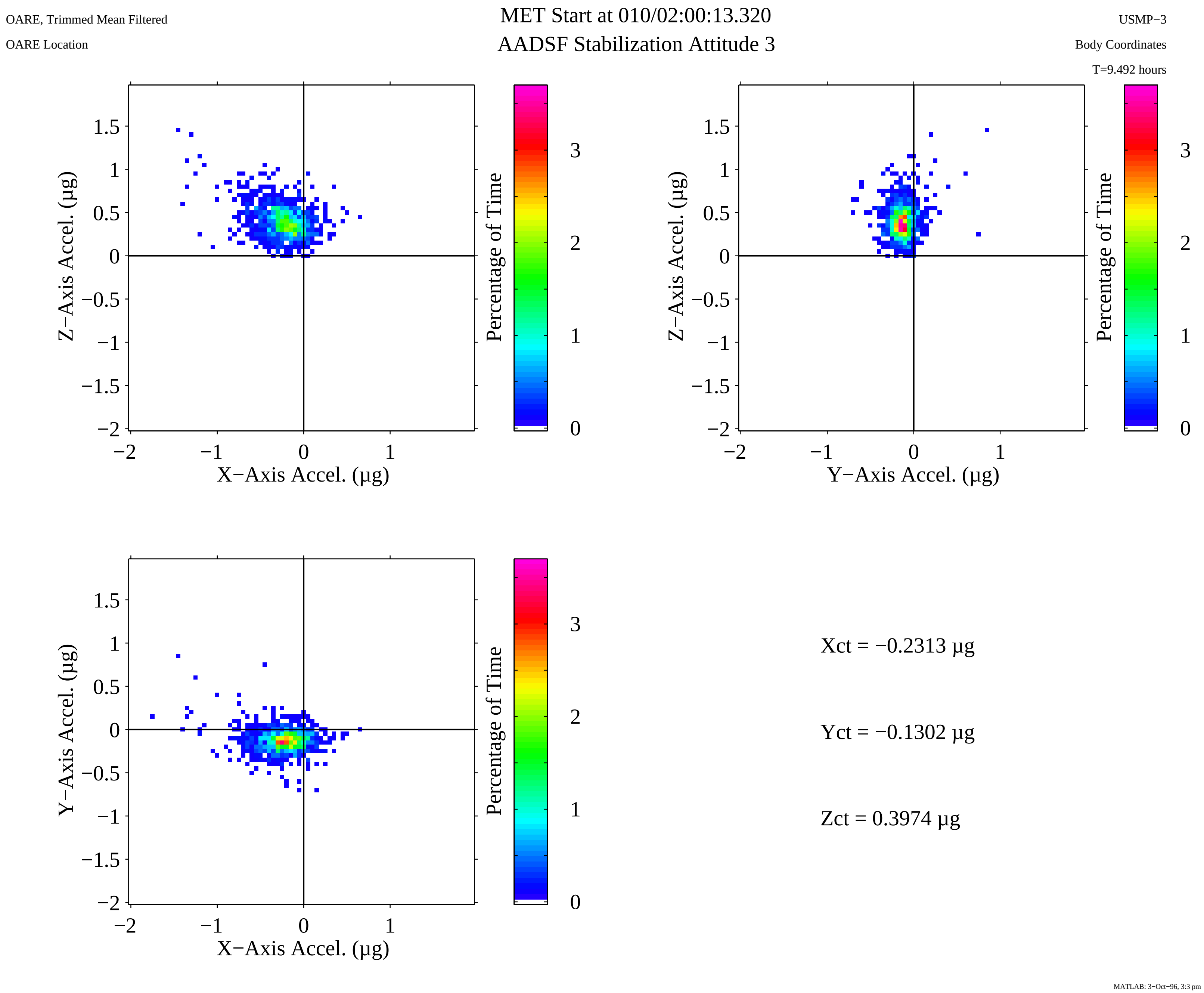

Fig. 27 Three-dimensional projection of the OARE data representing the microgravity environment at the OARE location while Columbia was in the AADSF 3 attitude. MET start at 010/02:00:13.

Appendix A: Accessing Acceleration Data via the Internet

SAMS and OARE data are available over the internet from the NASA LeRC file server "beech.lerc.nasa.gov". Previously, SAMS data were made available on CD-ROM, but distribution of data from current (and future) missions will be limited to the internet file server.

SAMS data files are arranged in a standard tree-like structure. Data are first separated based upon mission. Then, data are further subdivided based upon some portion of the mission, head, year (if applicable), day, and finally type of data file (acceleration, temperature, or gain). The following figure illustrates this structure.

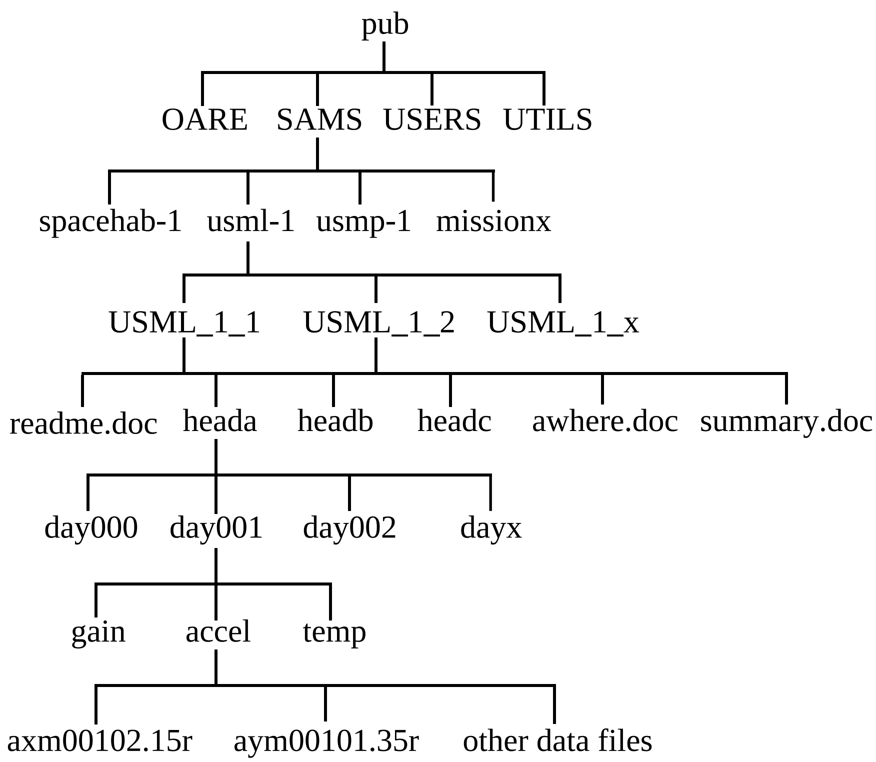

The SAMS data files (located at the bottom of the tree structure) are named based upon the contents of the file. For example, a file named "axm00102.15r" would contain head A data for the x-axis for day 001, hour 02, file 1 of 5. The readme.doc files give a complete explanation of the file naming convention.

For the USMP-3 mission, there are three entries at the "mission" level: USMP-3F, USMP-3G-Optical, and USMP-3G-Downlink. The optical and downlink data were kept separate for Unit G because of overlaps between recorded and telemetered data. Due to this overlap, data files with the same name may appear in both the Optical and Downlink branches.

OARE data files are also arranged in a tree-like structure, but with different branches. The data are first divided based upon mission, and then are divided based upon type of data. The OARE tree structure looks like this:

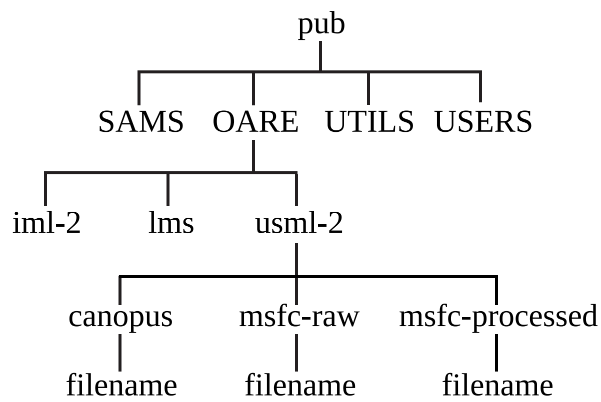

Files under the canopus directory are trimmean filter data, computed by Canopus Systems, Inc. Files under the msfc-raw directory contain the telemetry data files provided to PIMS by the Marshall Space Flight Center Payload Operations Control Center data reduction group. Files under the msfc-processed directory are raw files containing binary floating point values, listing the MET (in hours), and the x, y, and z axis acceleration in micro-g's. See the readme files for complete data descriptions.

Data access tools for different computer platforms (MS-DOS, Macintosh, SunOS, and MS-Windows) are available in the /pub/UTILS directory.

The NASA LeRC beech file server can be accessed via anonymous File Transfer Protocol (ftp), as follows:

1) Open a connection to "beech.lerc.nasa.gov"
2) Login as userid "anonymous"
3) Enter your e-mail address as the password
4) Change directory to pub
5) List the files and directories in the /pub directory
6) Change directories to the area of interest
7) Change directories to the mission of interest
8) Enable binary file transfers

9) Use the data file structures (described above) to locate the desired files
10) Transfer the desired files

If you encounter difficulty in accessing the data using the file server, please send an electronic mail message to “pims@lerc.nasa.gov”. Please describe the nature of the difficulty and also give a description of the hardware and software you are using to access the file server.

Appendix B: SAMS Time Histories and Color Spectrograms for Unit F

The Principal Investigator Microgravity Services (PIMS) group has processed SAMS data from STS-75, Unit F, Head 1B (fc=25 Hz, fs=125 samples per second) to produce the plots shown here. Three representations of the data are presented here: ten second interval average, ten second interval RMS, and PSD magnitude versus frequency versus time (spectrogram) plots. These calculations are presented in six hour plots, with the corresponding average and RMS plots on one page, and the spectrogram on the facing page.

The ten second interval average plots give an indication of net accelerations which last for a period of ten seconds or more. Shorter duration, high amplitude accelerations may be seen with this type of plot, however their exact timing and magnitude cannot be extracted. The ten second interval RMS plots give a measure of the oscillatory content in the acceleration data. Plots of this type may be used to identify times when oscillatory and/or transient deviations from the background acceleration levels occurred.

Color spectrograms are used to show how the microgravity environment varies in intensity with respect to both the time and frequency domains. These spectrograms are provided as an overview of the frequency characteristics of the SAMS data during the mission. Each spectrogram is a composite of six hour's worth of data. The time resolution used to compute the spectrograms seen here is 16.4 seconds. This corresponds to a frequency resolution of 0.06 Hz.

These data were collected at 125 samples per second, and a 25 Hz low pass filter was applied to the data by the SAMS unit prior to digitization. Prior to plot production, the raw SAMS data were compensated for gain changes, and then demeaned. Demeaning was accomplished by analyzing individual sections with a nominal length of 30 minutes. Users who are interested in further details for either of these operations are encouraged to contact the PIMS group.

Interval Average and Root Mean Square Calculations

The interval average plots were produced by calculating the average of ten second intervals of data for each axis.

This operation is described as: $x_{avg_k} = \frac{1}{M}\sum_{i=1}^{M} x_{(k-1)M+i}$,

where x represents the x, y, or z axis data, M is the number of points analyzed in an interval, and k refers to the kth interval analyzed.

The resulting data streams (x_{avg}, y_{avg}, z_{avg}) are then combined by a vector magnitude operation.

This computation is expressed mathematically as: $accel_{avg_k} = \sqrt{x^2_{avg_k} + y^2_{avg_k} + z^2_{avg_k}}$.

The interval RMS plots were produced by taking the root-mean-square of ten second intervals of data for each axis and forming a vector magnitude of the resulting data stream.

The interval RMS operation is expressed mathematically as: $x_{RMS_k} = \sqrt{\frac{1}{M}\sum_{i=1}^{M}\left(x_{(k-1)M+i}\right)^2}$.

The same definitions apply for x, M, and k as in the interval average computation. The resulting data streams are combined by a vector magnitude operation.

Power Spectral Density versus Frequency versus Time Calculations

In order to produce the spectrogram image, power spectral densities were computed for successive time intervals (the length of the interval is equal to the time resolution). For the PSD computation, a Hanning window was applied. In order to combine all three axes into a single plot to show an overall level, a vector magnitude (VM) operation was performed. Stated mathematically:

$$VM_k = \sqrt{PSD^2_{x_k} + PSD^2_{y_k} + PSD^2_{z_k}}.$$

By imaging the base 10 logarithm ($\log_{10}$) magnitude as a color and stacking successive PSDs from left to right, variations of acceleration magnitude and frequency are shown as a function of time. Colors are assigned to discrete magnitude ranges, so that there are 64 colors assigned to the entire range of magnitudes shown.

The colorbar limits are chosen in order to maximize the data value and visibility in a given set of spectrogram plots. Data which fall outside of these limits will be imaged as either the highest or lowest magnitude, depending on which side they have saturated. If an area of interest seems to be saturated, care should be taken because the actual values may lie above or below the color mapping shown on the plot.

Due to the nature of spectrograms, care should be taken to not merely read a color's numeric value as being the "amount" of acceleration that is present at a given frequency. In order to get this type of information, the PSDs must be integrated between two frequencies. These frequencies (lower and upper) form the band of interest. The result of this integration is the g_{RMS} acceleration level in the $\left[f_{lower}, f_{upper}\right]$ band. The PIMS group is able to provide this type of analysis on a per-request basis.

Plot gaps (if any exist) are shown by either white or dark blue areas on the page. If a plot gap exists for an entire plot (or series of successive plots), a comment is placed on the page to let the user know there is a gap in the data. These “no data available” comments will not show exact times for which the data are not available, but will only indicate missing plots.

Contacting PIMS

To request additional analysis or information, users are encouraged to send an e-mail to pims@lerc.nasa.gov, or FAX a request to (216) 433-8545.

Appendix C SAMS Time Histories and Color Spectrograms for Unit G

The Principal Investigator Microgravity Services (PIMS) group has further processed SAMS data from STS-75, Unit G, Head 2C (fc=25 Hz, fs=125 samples per second) to produce the plots shown here. Three representations of the data are presented here: ten second interval average, ten second interval RMS, and PSD magnitude versus frequency versus time (spectrogram) plots. These calculations are presented in six hour plots, with the corresponding average and RMS plots on one page, and the spectrogram on the facing page.

The ten second interval average plots give an indication of net accelerations which last for a period of ten seconds or more. Shorter duration, high amplitude accelerations may be seen with this type of plot, however their exact timing and magnitude cannot be extracted. The ten second interval RMS plots give a measure of the oscillatory content in the acceleration data. Plots of this type may be used to identify times when oscillatory and/or transient deviations from the background acceleration levels occurred.

Color spectrograms are used to show how the microgravity environment varies in intensity with respect to both the time and frequency domains. These spectrograms are provided as an overview of the frequency characteristics of the SAMS data during the mission. Each spectrogram is a composite of 6-hour's worth of data. The time resolution used to compute the spectrograms seen here is 16.384 seconds. This corresponds to a frequency resolution of 0.0610 Hz.

These data were collected at 125 samples per second, and a 25 Hz low pass filter was applied to the data by the SAMS unit prior to digitization. Prior to plot production, the raw SAMS data were compensated for gain changes, and then demeaned. Demeaning was accomplished by analyzing individual sections with a nominal length of 30 minutes. Users who are interested in further details for either of these operations are encouraged to contact the PIMS group.

Interval Average and Root Mean Square Calculations

The interval average plots were produced by calculating the average of ten second intervals of data for each axis.

This operation is described as: $x_{avg_k} = \frac{1}{M}\sum_{i=1}^{M} x_{(k-1)M+i}$,

where x represents the x, y, or z axis data, M is the number of points analyzed in an interval, and k refers to the kth interval analyzed.

The resulting data streams (x_{avg}, y_{avg}, z_{avg}) are then combined by a vector-magnitude operation.

This computation is expressed mathematically as: $accel_{avg_k} = \sqrt{x^2_{avg_k} + y^2_{avg_k} + z^2_{avg_k}}$.

The interval RMS plots were produced by taking the root-mean-square of ten second intervals of data for each axis and forming a vector magnitude of the resulting data stream.

The interval RMS operation is expressed mathematically as: $x_{RMS_k} = \sqrt{\frac{1}{M}\sum_{i=1}^{M}\left(x_{(k-1)M+i}\right)^2}$.

The same definitions apply for x, M, and k as in the interval average computation. The resulting data streams are combined by a vector-magnitude operation.

Power Spectral Density versus Frequency versus Time Calculations

In order to produce the spectrogram image, Power Spectral Densities were computed for successive time intervals (the length of the interval is equal to the time resolution). For the PSD computation, a Hanning window was applied. In order to combine all three axes into a single plot to show an overall level, a Vector-Magnitude (VM) operation was performed. Stated mathematically:

$$VM_k = \sqrt{PSD^2_{x_k} + PSD^2_{y_k} + PSD^2_{z_k}}.$$

By imaging the base 10 logarithm ($\log_{10}$) magnitude as a color and stacking successive PSDs from left to right, variations of acceleration magnitude and frequency are shown as a function of time. Colors are assigned to discrete magnitude ranges, so that there are 64 colors assigned to the entire range of magnitudes shown.

The colorbar limits are chosen in order to maximize the data value and visibility in a given set of spectrogram plots. Data which fall outside of these limits will be imaged as either the highest or lowest magnitude, depending on which side they have saturated. If an area of interest seems to be saturated, care should be taken in that the actual values may lie above or below the color mapping shown on the plot.

Due to the nature of spectrograms, care should be taken to not merely read a color's numeric value as being the "amount" of acceleration that is present at a given frequency. In order to get this type of information, the PSDs must be integrated between two frequencies. These frequencies (lower and upper) form the "band" of interest. The result of this integration is the g_{RMS} acceleration level in the $\left[f_{lower}, f_{upper}\right]$ band. The PIMS group is able to provide this type of analysis on a per-request basis.

Plot gaps (if any exist) are shown by either white or dark blue areas on the page. Care should be taken to not mistake a plot gap (represented by a black vertical band) with a quiet period. If a plot gap exists for an entire plot (or series of successive plots), a comment is placed on the page to let the user know there is a gap in the data. These “no data available” comments will not show exact times for which the data are not available, but will only indicate missing plots.

Contacting PIMS

To request additional analysis or information, users are encouraged to send an e-mail to pims@lerc.nasa.gov, or FAX a request to (216) 433-8545.

Appendix E User Comment Sheet

We would like you to give us some feedback so that we may improve the Mission Summary Reports. Please answer the following questions and give us your comments.

1. Do the Mission Summary Reports fulfill your requirements for acceleration and mission information?
______Yes ______No If not why not?

Comments:
____
____

2. Is there additional information which you feel should be included in the Mission Summary Reports?
______Yes ______No If so what is it?

Comments:
____
____

3. Is there information in these reports which you feel is not necessary or useful?

______Yes ______No If so, what is it?

Comments:
____
____

4. Do you have internet access via: (____)ftp (____)WWW (____)gopher (____)other? Have you already accessed SAMS data or information electronically?

______Yes ______No

Comments:
____
____

Completed by: Name:__________________________ Telephone______________________

Address:__________________________ Facsimile______________________

__________________________ E-mail addr______________________

Return this sheet to:
Duc Troung
NASA Lewis Research Center
21000 Brookpark Road MS 500-216
Cleveland, OH 44135

or
FAX to PIMS Project: 216-433-8660
e-mail to: pims@lerc.nasa.gov.